CHAPTER V

RADIOFREQUENCY SIZE EFFECTS IN METALS

BY

V. F. GANTMAKHER

INSTITUTE OF SOLID STATE PHYSICS,
ACADEMY OF SCIENCES OF THE USSR, MOSCOW

1. Introduction

In recent years quite a number of phenomena well described by the classical concept of electron trajectories have been discovered in the field of physics of metals. A number of quantum mechanical operations were realized while constructing the theory: a gas of elementary excitations (quasi-particles known as "electrons") that complies with a complicated dispersion which is related to reflecting the symmetry of a crystal lattice, is introduced and use is made of the Fermi statistics leading to the concept of Fermi surfaces. Then, in quite a number of cases, the movement of a quasi-particle-electron may be considered as classical with the use of such conceptions as the electron trajectories, effective mass m, mean free path l, character of scattering at metal surfaces, etc. It may be easily shown (see for example the discussion in Ref. 1) that such a consideration is valid up to those magnetic fields at which the distance between quantum energy levels is still very small as compared with characteristic energies of the dispersion law. At the same time the sample size should considerably exceed interatomic distances. Such a semi-classical approach requires sometimes (as in the case of magnetic breakdown, for example) additional quantum considerations. Nevertheless it is the main way of describing all the phenomena concerning kinetic processes.

The Azbel–Kaner cyclotron resonance presents a typical example of the quasi-classical effect. The classical concepts are quite adequate to describe it:

References p. 232

an electron moving within a magnetic field H, applied parallel to the surface of the metal, repeatedly returns to the skin layer every time finding the field near the surface in one and the same phase, if the condition $\omega = n\Omega$ is satisfied (ω is the frequency of the incident radio wave, $\Omega = eH/mc$ is the cyclotron frequency of the electron, n is an integer).

The radiofrequency size effects described in the present article also belong to this same category of phenomena. Let us consider a plane–parallel metal plate of thickness d experiencing the influence of an electromagnetic incident wave. The following inequality should be satisfied

$$\delta \ll d \ll \ell, \tag{1}$$

where δ is the skin-layer depth. When a constant magnetic field is applied to the plate, the straight electron trajectories change into complicated space curves. In case of a spherical Fermi surface, for example, circle and helical trajectories occur. The specific parameters of these curves (such as circle diameter, pitch of helical line, etc.) are inversely proportional to the magnitude of the magnetic field. It can be expected, naturally, that for such values of the field when these sizes become equal to d some singularities may occur in the surface impedance of the plate.

Size effects in direct current conductivity were discovered a long time ago[4]. The first of them was the increase of electrical resistance of a thin film as compared with the resistance of a bulk metal due to restriction of the electron free path l by the sample dimensions[9, 10]. Furthermore, there are a number of cases in the magnetoresistance of thin samples where the resistance decreases as the magnetic field increases[11], while for bulk metal the increase of the field leads usually to the increase of the resistance. This phenomenon occurs due to the twisting of the electron trajectories: an average drift of an electron in the magnetic field for the time of free path $t_p = l/v$ is found to be much smaller than the value of l and accordingly the influence of the sample boundaries becomes of little importance. Thus, as the field is increased, the difference between the thin and bulk samples should diminish. The resistance of a sample in the form of a plane–parallel plate in the magnetic field H applied perpendicular to the sample surface has an oscillating character[12–14]. The helical trajectory of the electron moving from one surface of the plate to the other is cut off at some turn fraction depending on the value of H. The magnitude of this fraction determines the oscillating component of the current.

If a supplementary small parameter with the dimensions of length exists in the experiment, the size effect may become more distinct. Sharvin and

References p. 232

Fisher[15], for example, in their recent experiments obtained a more distinct direct current size effect owing to the fact that the current was injected into and removed from the sample through thin points having a diameter ranging from 10^{-5} to 10^{-4} cm. An "electron beam" in the metal interior was focussed from one thin point to the other with the aid of a magnetic field.

In the case of radiofrequencies, the skin-layer depth δ is such a small parameter that more pronounced size effects are found in the impedance changes within narrow spaces of the fields ($\Delta H/H \sim \delta/d$). To explain causes of this phenomenon let us turn to the theory of the anomalous skin-effect.

2. Principles of the theory

2.1. Anomalous skin-effect in zero magnetic field

As it is well known there are two different approaches to the problem of the anomalous skin-effect which, generally speaking, do not compete with one another. The first entirely qualitative approach was developed by Pippard[16,17], who based his theory on rather fine conceptions known under the name of "ineffectiveness concept". Pippard suggested that an effective contribution to the skin-current is made only by those electrons which spend most part of the time between collisions in the skin layer. The velocity of such electrons forms with the surface angles less than δ/l. The remaining electrons leave the skin layer too fast and therefore the electric field has no time to affect them. Thus, it is possible to distinguish at the Fermi surface the effective region having the width δ/l and located along the line $\boldsymbol{vn}=0$ ($\boldsymbol{v}$ is the electron velocity, $\boldsymbol{n}$ is the normal to the metal surface). Then the effective electron ratio amounts to the order of magnitude δ/l. Introducing the effective conductivity $\sigma_{\text{eff}}=(\delta^*/l)\,\sigma_0$ instead of the static conductivity σ_0 into the well-known formulae for the surface impedance $Z=R+\mathrm{i}X$ and the complex penetration depth at normal skin-effect

$$Z=\frac{1}{c}\left(\frac{4\pi\omega}{\sigma_0}\right)^{\frac{1}{2}}\mathrm{e}^{\frac{1}{4}\mathrm{i}\pi}, \tag{2}$$

$$\delta^*=(c^2/4\pi\mathrm{i}\omega)\,Z, \tag{3}$$

we obtain

$$Z=2\left(\frac{2\pi^2\omega^2 l}{c^2\sigma_0}\right)^{\frac{1}{3}}\mathrm{e}^{\frac{1}{3}\mathrm{i}\pi}. \tag{4}$$

[Formula (3) introduced the complex value δ^*. Later, the symbol δ will be used for the real part of this value.]

The second approach to the problem of the anomalous skin-effect suggests a strictly mathematical solution of the problem of the propagation of electromagnetic waves in metals, when the current value at a given point is determined by the field distribution in the vicinity of the point having an electron free-path size. For the first time this problem was solved for a metal in zero magnetic field by Reuter and Sondheimer[18]. Their approach required the solution of a system of equations comprising Maxwell's equations, Boltzmann's kinetic equation for the distribution function of the electrons f depending on coordinate $\boldsymbol{r}$, momentum $\boldsymbol{p}$ and time t

$$\frac{\mathrm{d}f}{\mathrm{d}t} \equiv \frac{\partial f}{\partial t} + \dot{\boldsymbol{p}} \frac{\partial f}{\partial \boldsymbol{p}} + \dot{\boldsymbol{r}} \frac{\partial f}{\partial \boldsymbol{r}} = \left(\frac{\mathrm{d}f}{\mathrm{d}t}\right)_{\mathrm{coll}}, \tag{5}$$

and the expression for the current density $\boldsymbol{j}(\boldsymbol{r})$ at the given point

$$\boldsymbol{j}(\boldsymbol{r}) = \frac{2e}{h^3} \int (f - f_0) \boldsymbol{v}\, \mathrm{d}^3 p. \tag{6}$$

Here, f_0 is the equilibrium distribution function, and h is Planck's constant. Eqs. (5) and (6) substitute for Ohm's law $\boldsymbol{j} = \sigma_0 \boldsymbol{E}$. It is convenient to write the solution of these equations with respect to $\boldsymbol{j}(\boldsymbol{r})$ in the form suggested by Chambers[19]. For an unbounded metal this solution can be represented in the form

$$\boldsymbol{j}(\boldsymbol{r}_0, t_0) = -\frac{2e^2}{h^3} \int \mathrm{d}^3 p\, \boldsymbol{v} \frac{\partial f_0}{\partial \varepsilon} \int_{-\infty}^{t_0} \mathrm{d}t\, \boldsymbol{E}(\boldsymbol{r}_p, t)\, \boldsymbol{v}_p(t)\, \mathrm{e}^{-(t_0 - t)\nu}, \tag{7}$$

where ε is the electron energy, $\boldsymbol{E}$ is the electrical field vector, functions $\boldsymbol{v}_p(t)$ and $\boldsymbol{r}_p(t) = \boldsymbol{r}_0 + \int_{t_0}^{t} \boldsymbol{v}_p\, \mathrm{d}t = \boldsymbol{r}_p(\boldsymbol{r}_0, t_0, t)$ describe the trajectory along which the electron with momentum $\boldsymbol{p}$ arrives at point $\boldsymbol{r}_0$, and the frequency ν of collisions between electrons and scatterers is assumed to be independent of $\boldsymbol{p}$. The meaning of expression (7) can be easily explained in the following way. The electron is scattered into the trajectory $\boldsymbol{r}_p$ at the moment t previous to t_0. It is assumed that immediately after collisions the distribution function of the electrons is an equilibrium function and corresponds to an energy $\varepsilon - \Delta\varepsilon$, where $\Delta\varepsilon$ is the energy acquired by the electron from the applied electric field during the time interval (t, t_0) while moving along the trajectory. The addition to the distribution function which is of interest to us is equal to $f_0(\varepsilon - \Delta\varepsilon) - f_0(\varepsilon) = -(\partial f_0/\partial\varepsilon)\Delta_p$. The integration over $\mathrm{d}^3 p$ in (7) covers all the possible trajectories passing through the point r_0, while the second integral

References p. 232

determines a magnitude of the addition $f_1 = f - f_0$ along each of these trajectories (the factor $\exp\{-(t_0 - t)\nu\}$ is the probability that the electron will reach the point r_0 without collisions).

In the case of a bounded metal some of the trajectories passing through r_0 originate on the surface; the lower limit $-\infty$ of the second integral converts into $t_s(\boldsymbol{p})$. Introducing (7) into Maxwell's equations we arrive at an integral–differential equation the solution of which for a half-space is described in Ref. 18.

The results[18] are well known. The attention should be drawn to only one of them which will be referred to below. Under conditions of anomalous skin-effect it is impossible to describe the field in a metal with the aid of a damped exponential wave[5,20]. The precise expression for the field contains two components. One of them is connected with effective electrons and describes a sharp decrease of the field near a metal surface. The other component caused by ineffective electrons has the form $e^{-\xi}/\xi^2$ (where $\xi = z/l$, z is the distance from the surface). This component is small, but it damps relatively slowly. In view of such a complicated form of field damping, the value δ which figures in the ineffectiveness concept should be strictly determined. We have taken the value δ from relation (3) though it differs, of course, from the distance at which the field becomes practically zero[5]. In any case, it is just this value (3) which is determined by the measurements[21-25] of R and X.

2.2. Anomalous skin-effect in a magnetic field

In the case of radiofrequency size effects, which is of interest to us, an additional constant magnetic field is applied to a metal. The criterion of skin-effect anomaly in the presence of the magnetic field is as follows

$$\delta \ll D, \tag{8}$$

where D is the characteristic size of the electron trajectories.

Let us consider the modification of both approaches to the anomalous skin-effect in the presence of a constant magnetic field. Since the shape of electron trajectories will be often dealt with below, it is useful to mention the possible forms of electron trajectories in a magnetic field when the free path is sufficiently long. The integrals of the equations of motion

$$\dot{\boldsymbol{p}} = (e/c)[\boldsymbol{v}\boldsymbol{H}], \qquad \boldsymbol{v} = \partial\varepsilon/\partial\boldsymbol{p} \tag{9}$$

have the form

$$\boldsymbol{p}_H = \text{const.}, \qquad \varepsilon = \text{const.} \tag{10}$$

References p. 232

It means that in momentum space an electron travels along the line of intersection of the isoenergetic surface $\varepsilon = \text{const.}$ with a plane normal to the direction of field $\boldsymbol{H}$. (To avoid misunderstanding we shall use below the term "orbit" for an electron movement in the momentum space.) As the left part of eq. (9) is the velocity along the $\boldsymbol{p}$-orbit and the right part of this equation contains the velocity along the $\boldsymbol{r}$-trajectory, it can be seen from eq. (9) that the electron orbit in momentum space ($\boldsymbol{p}$-space) and the projection of the electron trajectory in the $\boldsymbol{r}$-space on a plane perpendicular to $\boldsymbol{H}$ are similar to the similarity factor eh/c and are rotated relative to each other through the angle $\frac{1}{2}\pi$. A set of electron orbits exists for every direction of a magnetic field, as the p_H may assume any magnitude within the Brillouin zone (the energy ε is fixed and equal to the Fermi energy ε_F). The corresponding trajectories may be closed, helical and open ones. The closed trajectories correspond usually to cross-sections of the Fermi surface containing a centre of symmetry. It should be noted that these trajectories are not necessarily lying within the plane which is perpendicular to $\boldsymbol{H}$ and, in general, they are not necessarily in the shape of flat curves. The helical trajectories are obtained in the case of non-central closed orbits. The mean velocity $\bar{v}$ along these trajectories is parallel to $\boldsymbol{H}$ and the pitch depends on p_H. In the vicinity of the elliptical limiting points where the plane perpendicular to $\boldsymbol{H}$ touches the Fermi surface (the orbit degenerates to a point and the trajectory becomes a straight line) the pitch and period of motion in time are the same for all helical trajectories. The open trajectories exist only in metals with open Fermi surfaces, but not for all directions of the magnetic field. The main feature of these trajectories is that the motion is infinite in the plane perpendicular to $\boldsymbol{H}$. There are also trajectories with self-intersections[1,2] corresponding to isolated values of p_H but we will not discuss them here. The particular set of trajectories is determined, of course, by the Fermi surface and the direction of $\boldsymbol{H}$ relative to the crystallographic axis.

Let us return to eq. (7). In the presence of a constant magnetic field the equation remains valid, since this field changes only the electron trajectories and this is taken into account in the functions $\boldsymbol{r}_{\boldsymbol{p}}(t)$ and $t_s(\boldsymbol{p})$. But the integration in (7) becomes more complicated. The method of solving the problem of the anomalous skin-effect in the presence of a magnetic field was worked out by Azbel and Kaner[26-28]. The scheme of their method may be described in the following way (see also Refs. 6 and 7).

Let a half-space $z>0$ be filled with a metal and have an electromagnetic wave $\boldsymbol{E}e^{-i\omega t}$ falling upon it from the outside. In the cases which are of interest to us it is possible to neglect the component of field E_z in a metal along the

References p. 232

normal Oz[7,27]. Maxwell's equations in this case may be reduced to the following two equations

$$\frac{\partial^2 E_\alpha}{\partial z^2} = -\frac{4\pi i\omega}{c^2} j_\alpha(z), \qquad \alpha = x, y. \tag{11}$$

The problem of a half-space is then replaced with the problem of a whole space excited "from the inside" in the plane $z=0$. For this purpose the field and the current are continued in an even fashion into the region $z<0$: $\boldsymbol{E}(-z)=\boldsymbol{E}(z)$. From eq. (7) for the current which should be solved together with eqs. (11), this operation means that we change boundary conditions for the distribution function and use again $-\infty$ as the lower limit in the intrinsic integral of eq. (7). As it can be seen in Fig. 1, this is not equivalent to the case

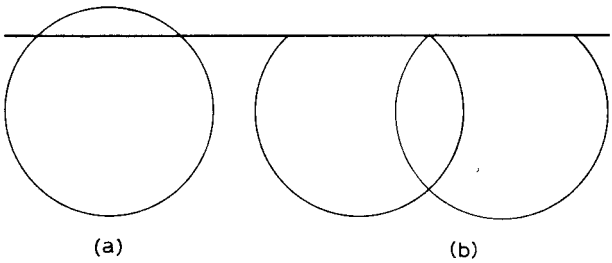

Fig. 1. Electron trajectories in a magnetic field: (a) at formal even extension of the electric field to the region $z<0$; (b) at specular scattering.

of specular scattering of electrons at the surface. This operation means rather that we have completely neglected the scattering at the surface. The odd extension of the field and currents to the region $z<0$ may be used with the same success[3].

A basis for neglecting the boundary can be found in the work of Reuter and Sondheimer[18]. Their results show that in zero magnetic field the character of scattering at the surface only slightly influences the impedance value. A similar result was obtained for the case of anomalous skin-effect in a magnetic field[26], when the problem of the cyclotron resonance was solved for the case of diffuse scattering (see also below, p. 192).

The transition from the half-space to the whole space makes it possible to use the Fourier transformation for the solution of eqs. (11). Using plane waves with wave vector along the z axis one may draw the following formal

relationship

$$\mathscr{J}_\alpha(k) = \sigma_{\alpha\beta}(k)\,\mathscr{E}_\beta(k), \tag{12}$$

between the Fourier components of the electric field

$$\mathscr{E}_\alpha(k) = 2\int_0^\infty E_\alpha(z)\cos kz\,\mathrm{d}z \tag{13}$$

and those of the current

$$\mathscr{J}_\alpha(k) = 2\int_0^\infty j_\alpha(z)\cos kz\,\mathrm{d}z$$

[in eq. (12) the summation over index β is supposed]. In the result of the Fourier transformation the differential equations for $E(z)$ are replaced with the algebraic equations for $\varepsilon(k)$ which can be readily solved. The result of the solution is

$$\mathscr{E}_\alpha(k) = -2\left[k^2\hat{I} - 4\pi i\omega c^{-2}\hat{\sigma}(k)\right]^{-1}_{\alpha\beta}E'_\beta(0), \tag{14}$$

where $\hat{I}$ is the unit matrix, $\hat{\sigma}(k)$ is the conductivity tensor introduced by eq. (12) and the prime denotes the derivative with respect to z. In many problems the x and y axes may be chosen. in such a way that the non-diagonal components of the tensor become equal to zero and as a result eq. (14) takes the form:

$$\mathscr{E}_\alpha(k) = \frac{-2E'_\alpha(0)}{k^2 - 4\pi i\omega c^{-2}\sigma_\alpha(k)}, \qquad \alpha = x, y. \tag{15}$$

(The term $-2E'(0)$ appears in eqs. (14) and (15) due to the fact that in the case where the field is evenly continued into the region $z<0$ the derivative $\partial E/\partial z$ has a discontinuity at the plane $z=0$.) The problem is brought now to the calculation of the tensor $\sigma_{\alpha\beta}(k)$.

The meaning of the operations carried out up to now is as follows. The sharp inhomogeneity of the field near the surface of the metal is presented in a form of superposition of monochromatic plane waves $\mathscr{E}(k)\,\mathrm{e}^{-i\omega t}\cos kz$, where ω is the frequency of the external wave and the wave vectors k form a continuous spectrum with the width $\Delta k \sim \delta^{-1}$. Now it is necessary to determine the relationship between the field and the current for such monochromatic waves only.

Up to now we have used Maxwell's equations only. To determine the

References p. 232

function $\sigma(k)$ it is necessary to use the kinetic equation. We have to introduce the field in the form of the monochromatic wave

$$E_k(z) = \mathscr{E}(k)\, e^{-i\omega t} \cos kz \tag{16}$$

into the expression for the current (7) and to take into account the shape of the electron trajectories.

For consideration of the electron trajectories it is convenient to use variables in the momentum space suggested in Ref. 29: the energy ε, the momentum component along the field p_H and the dimensionless time τ. The first two variables are, as is clear from (10), the integrals of motion determining the electron orbit in the momentum space, while τ determines the position of an electron in the orbit (phase of motion). The quantity $\tau = \Omega t$, where t is the time of electron motion in the orbit measured from an arbitrary initial moment. The integration over d^3p in eq. (7) implicates the integration over all the trajectories passing through the point r_0. After replacement of $d^3p = |m|\, d\varepsilon\, dp_H\, d\tau$, the integration over $d\varepsilon$ and dp_H implicates the use of all the possible orbits and $\int_0^{2\pi} d\tau$ means the integration over all the trajectories corresponding to a definite orbit and passing through the point τ_0 (see also Refs. 7 and 28).

Introducing the electric field expressed in the form (16) into the integrand of eq. (7), we obtain for $\boldsymbol{E}$ for example parallel to x:

$$Y(z_0, t_0) = \int_{-\infty}^{t_0} dt\, E_x(z,t)\, v_x(t) \exp\{-(t_0 - t)\nu\} =$$

$$= \frac{\mathscr{E}_x(k) \exp(-i\omega t_0)}{\Omega} \int_{-\infty}^{\tau} d\tau\, v_x(\tau) \exp\left\{-\frac{-i\omega + \nu}{\Omega}(\tau - \tau_0)\right\} \times$$

$$\times \cos k\left\{z_0 + \frac{1}{\Omega}\int_{\tau_0}^{\tau} v_z(\tau')\, d\tau'\right\}. \tag{17}$$

Decomposing the cosine sum into two components we leave only the even term $\cos kz_0 \cos\{(k/\Omega)\int v_z\, d\tau\}$ in accordance with the previously chosen continuous extention of the current to the region $z<0$*. Introducing (17) into (7) and taking into account (12), we finally obtain the following general

* The term with the product of the sines when integrating over d^3p would become zero due to the central symmetry of the Fermi surfaces. It is just this symmetry that permits us to introduce even extensions for $\boldsymbol{E}$ and for $\boldsymbol{j}$ simultaneously.

References p. 232

expression for $\sigma_{\alpha\beta}(k)$

$$\sigma_{\alpha\beta}(k) = \frac{2e^2}{k^3} \int_0^{\infty} -\left(\frac{\partial f_0}{\partial \varepsilon}\right) d\varepsilon \int \frac{m\, dp_H}{\Omega} \int_0^{2\pi} d\tau_0\, v_\alpha(\tau_0) \times$$

$$\times \int_{-\infty}^{\tau} d\tau\, v_\beta(\tau) \exp\left\{\frac{\nu - i\omega}{\Omega}(\tau_0 - \tau)\right\} \cos\left\{\frac{k}{\Omega}\int_{\tau}^{\tau_0} v_z(\tau')\, d\tau'\right\}. \quad (18)$$

It is expression (18) that is used at the initial stage for each particular calculation. After the $\sigma_{\alpha\beta}(k)$ is determined for the particular conditions of the problem, such as the range of frequencies ω, the magnitude of the magnetic field and its direction relative to the surface, the shape of the Fermi surface, etc., the field is determined according to the common formula

$$E_\alpha(z) = \frac{1}{\pi} \int_0^{\infty} \mathscr{E}_\alpha(k) \cos kz\, dz, \quad (19)$$

where $\mathscr{E}_\alpha(k)$ is obtained with the use of expressions (14) or (15).

There is, however, another operation which is common for all particular calculations. Since $k \sim \delta^{-1}$, the expression under the cos in eq. (18) may have, according to the condition (8), large values and, hence, $\cos kz(\tau_0, \tau)$ is a rapidly oscillating function. In other words, the trajectory encompasses many wave lengths and the phase of the electric field along the trajectory is rapidly oscillating. As a result it is possible to use the stationary-phase method for the calculation of the integrals over τ_0 and τ in eq. (18). The use of the phase–amplitude diagram and Cornu spirals suggested by Pippard[6] is essentially a graphic geometrical variant of the same method. The possibility of using the stationary-phase method means that the main contribution to $\sigma(k)$ is made by those parts of the electron trajectories where $z(\tau)$ takes a stationary value, i.e. by those parts which are near points $v_z = \Omega \partial z/\partial \tau = 0$. We again arrive at the "effective region" $v_z = 0$ on the Fermi surface and the "ineffectiveness concept" suggested by Pippard.

The effective region may intersect orbits of any type mentioned above and therefore one or several effective points with $v_z = 0$ may occur on each of the orbits. The width of the effective part τ_{eff} in the orbit may be determined from the ratio of the length of the trajectory part near an effective point for which the coordinate z change Δz is less than δ to the length of the trajectory travelled during the period $2\pi/\Omega$ ($\Delta\tau = 2\pi$).

References p. 232

As it can be seen from Fig. 2, for the closed orbits and for a field applied parallel to a metal surface, $\tau_{\text{eff}} \sim (\delta/R)^{\frac{1}{2}}$, where R is the radius of curvature of the trajectory near an effective point. Thus, it turns out that τ_{eff} depends on p_H and H. As another example we may consider a helical trajectory in an inclined magnetic field. In a lateral projection the helical trajectories are of

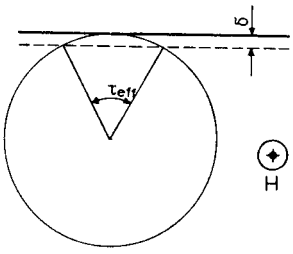

Fig. 2. A closed trajectory when $\boldsymbol{H}$ is parallel to the metal surface.

a sinusoidal shape. The sinusoidal curve shown in Fig. 3 has one point $v_z = 0$ through a period and at this point $\partial^2 z/\partial\tau^2 = 0$ too. It is easy to show that the length of the effective part of the trajectory is equal to $L = \partial^{\frac{1}{3}} u^{\frac{2}{3}} \varphi^{-1}$ and, therefore, $\tau_{\text{eff}} \sim (\delta/u)^{\frac{1}{3}}$ (angle φ is assumed to be small).

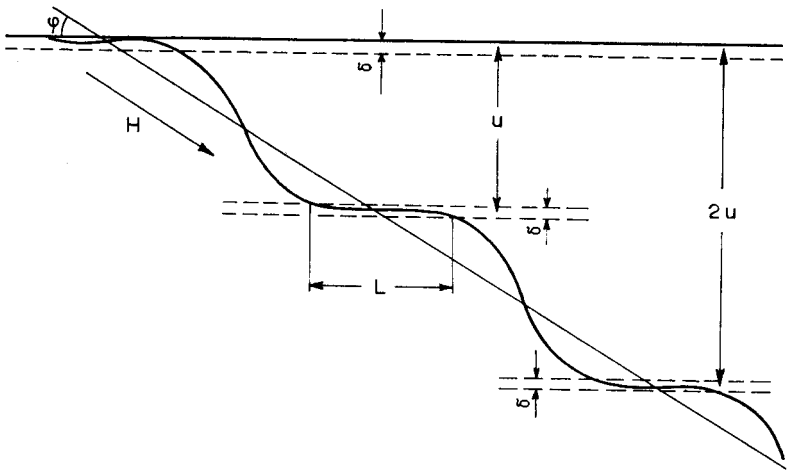

Fig. 3. A helical trajectory in an inclined magnetic field with one effective point through a period (a lateral projection).

References p. 232

The following important factor should be noted. The stationary-phase method is used twice for the calculation of $\sigma(k)$. The current at the given point z_0 is determined first by electrons having $v_z(z_0)=0$ [integration over orbit centres (over τ_0); see eq. (7)]. But among them the main contribution is made by those electrons which previously (when $\tau<\tau_0$) have passed effective points with $\partial z/\partial\tau=0$ in regions of values z where the field E differs from zero. So for the effectiveness of an electron at least two effective points in its trajectory are necessary.

In fact, the strict theory uses to some extent the ineffective concept too. The form of expression (18) reflects the fact that f_1 differs from zero along the effective region only, where $v_z\simeq 0$. This is the main argument in favour of the assumption that the scattering at the surface does not considerably influence the impedance of metal Z in a magnetic field because the electrons for which v_z is strictly equal to zero never collide with the surface. Nevertheless it should be borne in mind that the trajectories of the type shown in Fig. 4

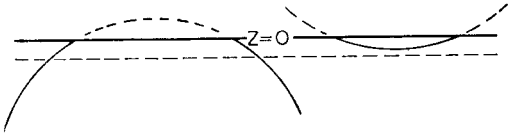

Fig. 4. Electron trajectories whose contribution to the skin current is essentially altered due to the existence of the metal surface.

have not been taken into account correctly. This is of little importance in the case of cyclotron resonance[26,27], since these trajectories do not determine the nature of the phenomenon. But for monotonic dependences $Z(H)$ in weak and strong fields (with $\Omega\ll\omega$ and $\Omega\gg\omega$) these trajectories may become significant. The problem about impedance changes in these regions is not clear yet, because the predicted behaviour of the impedance[27] is not yet confirmed experimentally[30-32].

The obtained form of function f_1 justifies also the replacement of the collision integral in expression (5) with the relaxation term $-f_1\nu$ (Ref. 26). It is the function f_1, but not f_0, which is important in the collision integral. Since $f_1\simeq 0$, far from the region $v_z=0$, the role of scattering processes reduces to the removal of some electrons from the number of effective electrons, while the replenishment at the expense of other electrons does not practically occur. In this respect the electrons on the effective trajectories are similar to particles in a beam: the only result of collisions is that they come out of the process.

References p. 232

(In the general case of anomalous skin-effect, v should be considered as a function of $\boldsymbol{p}$, but this assumption only slightly complicates the formulae given above[7,19].)

2.3. Application of the ineffectiveness concept to the study of size effects

The calculations of impedance in a magnetic field may be considerably facilitated by the use of the ineffectiveness concept. Heine[33] was the first who used the ineffectiveness concept for a problem with a magnetic field in an approximate theory of the cyclotron resonance. He determined approximately the current I in a skin layer with the aid of expression (7), introduced the value $\sigma_{\text{eff}} = I/E$, substituted it into eq. (2) and brought the problem to Pippard's scheme with another σ_{eff}.

Let us use the same scheme to show the existence of a radiofrequency size effect in a plane-parallel plate of thickness d under the following conditions: an electromagnetic wave $\boldsymbol{E}_0 e^{-i\omega t}$ falls upon one side of the plate and $\boldsymbol{E}_0 \| Oy$; a constant magnetic field is applied parallel to the surface, $\boldsymbol{H} \| Ox$; the dispersion law is a square and an isotropic one, $\varepsilon_F = p_0^2/2m$; the inequalities (1) are well satisfied and, besides,

$$\Omega \gg \nu \gg \omega . \tag{20}$$

The last inequalities mean that for the time of free path an electron makes several revolutions in the orbit, but it is possible to neglect the change of phase of the field in the skin layer for this period of time. These conditions may be practically satisfied if we take $\omega \lesssim 10^7$–10^8 sec^{-1}; $H \sim 10^2$–10^3 Oe at the free path $l \sim 10^{-1}$ cm; $\delta \sim 10^{-4}$ cm corresponds to these frequencies.

For an electron which passes repeatedly through the skin layer, the last integral in expression (7) is replaced with the geometric progression[33]

$$Y_1 = E_0 v_y \frac{\tau_{\text{eff}}}{\Omega} (1 + e^{-w} + e^{-2w} + \ldots) = \frac{E_0 v_y \tau_{\text{eff}}}{(1 - e^{-w})} . \tag{21}$$

Here, the factor

$$e^{-w} = e^{-2\pi\nu/\Omega} \simeq \left(1 - \frac{2\pi\nu}{\Omega}\right) \tag{22}$$

determines the change of the integrand in (7) for every other revolution of the electron. The ratio $\tau_{\text{eff}}/\Omega = \Omega^{-1}\sqrt{\delta/R(p_H)}$ is the time required for passing along the part of the trajectory within the skin layer. If after passing through

the skin layer the electron at its first revolution collides with the opposite side of the plate and scatters, only the first member

$$Y_2 = E_0 v_y \tau_{\text{eff}}/\Omega \tag{23}$$

will remain from Y_1. [We neglect numerical factors of the order of unity in expressions (21) and (23).] Considering $-\partial f_0/\partial\varepsilon$ as a δ-function and replacing the integration over τ_0 in accordance with the ineffectiveness concept with multiplication by τ_{eff}, we obtain the current in the skin layer

$$I = \frac{2e^2}{h^3}\int \mathrm{d}p_x\, m v_y(p_x)\tau_{\text{eff}} Y = \frac{2e^2}{h^3}\, E_0\delta\left(\frac{1}{w}\int_{p_1}^{p_0} p_y\,\mathrm{d}p_x + \int_0^{p_1} p_y\,\mathrm{d}p_x\right).$$

Neglecting the unit compared with $1/w$ we have

$$\sigma_{\text{eff}} = \frac{I}{E_0\delta} = \frac{e^2}{h^3}\frac{p_0^2}{w}\left(\tfrac{1}{2}\pi - \theta_1 - \tfrac{1}{2}\sin 2\theta_1\right), \tag{24}$$

where p_1 is the minimum value of the momentum component along the field at which the electron can still move within the plate and

$$\theta_1 = \arcsin(p_1/p_0) = \arccos(edH/2cp_0).$$

The differentiation of (24) with respect to H immediately shows that $\partial\sigma_{\text{eff}}/\partial H$ and, hence, $\partial Z/\partial H = (\partial Z/\partial\sigma_{\text{eff}})(\partial\sigma_{\text{eff}}/\partial H)$ become infinite at the point $H = H_0 = 2cp_0/ed$ on the left. H_0 is the value of the magnetic field at which the diameter of the electron trajectories belonging to the extreme Fermi sphere section becomes equal to the plate thickness.

This result may be commented with the use of the following simple considerations. The electrons move along helices with axes parallel to the surface of the metal; the major part of the electron trajectories passes deep in the metal where there is no high-frequency field ($\delta \ll D$); on returning to the skin layer, the electrons find there a high-frequency field in the same phase as it was during the preceding passage through the skin layer ($\omega \ll \Omega$). The dependence of the impedance on the field, however, does not have a resonance character, since the condition of constant phase of the electric field for all passages of the electron through the skin layer is fulfilled for all fields. When the field is decreased, the dimension of the electron trajectory increases and the number of returns of the electron through the skin layer during the free path time decreases. However, the electron returns to the skin layer only if the diameter of its trajectory is less than the thickness of the sample ($D \leq d$). When the opposite is true ($D > d$) the electron is scattered at the surface of

References p. 232

the plate. A comparatively large number of trajectories has the same value D_0 determined by the diameter of the Fermi sphere [the function $D(p_H)$ has an extremum at $p_H=0$]. Naturally, the function $Z(H)$ has a certain singularity for a corresponding value of the field H_0.

From the theoretical point of view the condition $\Omega \ll \omega$ is of little significance in this case. Replacing (20) with the relation

$$\Omega \sim \omega \gg \nu \tag{25}$$

we find that w in eqs. (21) and (22) becomes equal to

$$w = \frac{2\pi}{\Omega}(\nu - i\omega)$$

and we cannot use the expansion of e^{-w}. Under these conditions the discontinuity of the impedance derivative remains at $H=H_0$ (Ref. 34). Since the denominator $(1-e^{-w})$ is of resonance character with deep minima at $\omega=n\Omega$ $(n=1, 2, \ldots)$, equal to $2\pi\nu/\Omega$, this discontinuity occurs against the background of the cyclotron resonances.

There is one more effect in the frequency region (25). In the case of essentially a non-square dispersion law m is a function of p_H. The electrons participating in the cyclotron resonance are located in the momentum space near the extremal orbit and have the same trajectory size $D=2pc/eH$. When H is less than $H_0=2pc/ed$, these resonance trajectories do not pass into the plate and as a result the cyclotron resonances should vanish. This phenomenon, observed experimentally by Khaîkin[35] who called it "cyclotron resonance cut off", is the first one in the whole group of radiofrequency size effects discovered later on.

Such semi-qualitative calculations as those given above are of relatively small value. It is more important that the ineffectiveness concept determines the general approach to the whole group of problems, which is convenient for this field. Using the terms of this concept we shall show, for example, that in the presence of a magnetic field it is possible to observe the anomalous penetration of the electromagnetic field into a metal, resulting in field and current splashes deep inside the metal.

Let us consider a trajectory with one effective point (i.e. a point with $v_z=0$) within the skin layer, and the other points inside the metal. Such trajectories are shown, for example, in Figs. 2 and 3. An electron moving within the skin layer along such a trajectory obtains from the field the energy $\Delta\varepsilon \simeq Ev\tau_{\text{eff}}/\Omega$ [see eq. (23)] as well as the changes of momentum $\Delta p \sim \Delta\varepsilon/v$ and velocity $\Delta v \sim \Delta p/m$. For this reason the electron may be considered as a personifi-

cation of the non-equilibrium addition to the distribution function or, in other words, as a carrier of a part of the current $\Delta j \sim e\Delta v$ in the skin layer. As the electron moves along the trajectory, Δp and Δv somehow change. But at the next effective point of the trajectory, which is located deep in the metal out of the skin layer, the electron will move again parallel to the surface and will reproduce its change of velocity Δv and, hence, of the current Δj.

The value u, showing the displacement of the electron into the depth of the metal while travelling from one effective point to the other, depends on p_H. Therefore, different trajectories, which participate in the skin-layer current, have their effective points located at various depths. As a result the secondary current must, generally speaking, be diffused through a considerable depth. But at a depth u_{ext}, corresponding to the extremum of function $u(p_H)$, the number of effective trajectories increases sharply. It is obvious that a sharp increase (a splash) of current and electromagnetic field may also be expected at such depths.

These considerations are applicable to the trajectories of various types. In case of a square dispersion law and a magnetic field applied parallel to the metal surface, the splash should occur at a depth $D_0 = 2p_0c/eH$, due to orbits in the vicinity of the central section of the Fermi sphere. Since this splash is a peculiar skin layer for electrons rotating deep in the metal, it, in its turn, causes the next splash at a depth $2D_0$, etc. As a result, a system of splashes determined by the chain of electron trajectories will appear within the metal.

The splashes caused by helical trajectories in the vicinity of the limiting points in a slightly inclined magnetic field are formed in a somewhat different way. They are determined not by a chain of trajectories, but by one group of trajectories passing directly from the metal surface and having many effective points located at various depths (see Fig. 3).

The possibility of the existence of splashes was described for the first time by Azbel[28] and then the occurrence of splashes under various conditions was studied theoretically and experimentally by Kaner and the author[36-38], as well as by Kip and his collaborators[39]. Later on we will return to the splashes. Here we want to show only that size effects are tightly connected with the existence of splashes. Let us assume, indeed, for the sake of simplicity that $l \sim d \gg \delta$. Then in the case of a single-side excitation by an incident wave, the distribution of the field in the plate will coincide in a first approximation with the distribution in a semi-infinite metal. Since u_{ext} depends on H, by changing H we may change the depths of the location of splashes. It means

References p. 232

that a splash may be brought to the opposite surface of the plate from which the energy will be radiated into space. At certain values of the magnetic field the electromagnetic radiation can penetrate the metal plate.

Our considerations based on the "ineffectiveness concept" have already led us to several possibilities for a different size effect occurrence: the cutoff of trajectories, anomalous penetration of the field due to chains of trajectories and due to trajectories with $\overline{v_z} \neq 0$. Realizations of these possibilities are discussed in Sections 3.2–3.5. There is one more possibility related to a small slowly damping component of the field from the ineffective trajectories. (For instance, a helical trajectory is ineffective when $\boldsymbol{H} \| \boldsymbol{n}$.) Relations between the plate thickness d and the extremal ineffective electron trajectories may also lead to radiofrequency size effects. Such effects are described in Section 3.6.

3. Various types of radiofrequency size effects

3.1. Methods of detection of size effects

The experiments on the detection of the radiofrequency size effects may be approached from different sides not only in the figurative, but almost in the literal meaning of this expression. One of the possible approaches was realized by Khaîkin[35] at frequencies $f \sim 10^{10}$ c/s. The sample in the form of a disk was used as a wall of the resonator and therefore the characteristics of the sample were studied from the side of the same surface upon which an initial electromagnetic wave was falling.

Khaîkin[35] used a strip resonator ensuring linearity of H.F. currents on the sample surface[40]. This condition is very important for the study of physical properties of metals. The strip resonators have a comparatively small quality factor and this makes it difficult to use them in common radiospectrometers for the microwave range. This difficulty was overcome by the use of the frequency modulation method for which the generation frequency coincided with the natural resonance frequency and for which the imaginary part of the surface impedance $Z = R + iX$ was measured. The records illustrating the cyclotron resonance cutoff in tin are shown in Fig. 5. Later on the cyclotron resonance cutoff was observed also in bismuth[41] and indium[42]. In all these cases the Fermi surface differs considerably from the sphere and this facilitates the observation of the effect.

The experiments with the "single-side geometry" are badly adapted to the registration of the anomalous penetration of the field. To register from the side of the incident wave $z = 0$ the arrival of the splash to the opposite surface $z = d$, from the latter the "reflected signal" should return. As the electro-

magnetic waves cannot propagate within the metal in the usual way, this "signal" should return due to the action of the same splash mechanism with the help of electrons drifting to the surface $z=0$.

For this reason, for the observation of size effects related to the anomalous penetration, it is natural to measure the signal which has passed through the plate. Such a method of studying the size effect was used by Walsh and

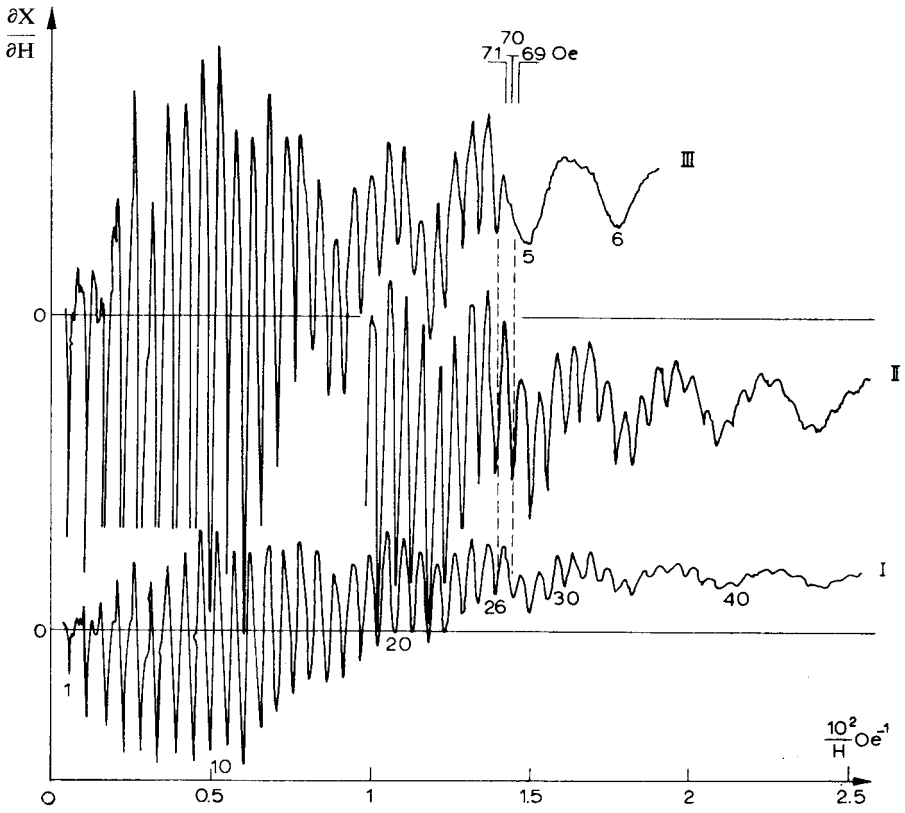

Fig. 5. A cutoff of the cyclotron resonances in tin[35]. Records on tin single crystals of thickness 2 mm (curves I and II, the latter with greater amplification) and of thickness 1 mm (curve III); $T = 3.75$ °K, $f \simeq 10$ Gc/s, $\boldsymbol{n} \parallel [100]$, $\boldsymbol{H} \parallel [001]$.

Grimes[43,44]. The transmitting coil excited by the radiofrequency generator was placed near one of the sample surfaces and the other similar coil at the opposite surface served as the receiver. The main experiments were carried out at a frequency of 4 Mc/s, but the frequency could be changed within a

References p. 232

wide range. Due to the modulation of the constant magnetic field and the use of a lock-in detector, just a part of the signal which passed through the sample could be selected (in principle the same scheme of experiment may be accomplished for the microwave range too[45, 46]).

At the same time there is another approach, which may be used for the observation of both the cutoff effects and the effects of the anomalous penetration. This approach is based on the double-side excitation of the plate with an electromagnetic wave. The major part of experiments in the field of the radiofrequency size effects was carried out with the help of such methods of excitation.

At high frequencies the excitation of this type takes place in those cases when the sample is placed in the centre of the resonant cavity (see Ref. 40 – the resonator with a rectangular sample with the size $13 \times 6\ \mathrm{mm}^2$). Such a resonator was used for the observation of the non-resonant orbit cutoff[47] (the impedance jump) for the same group of carriers in Sn for which the cyclotron resonance cutoff had been observed previously. A special thin sample with $d = 0.18$ mm was prepared for this experiment and as a result the cutoff field was displaced to the region of large fields. The intervals between the cyclotron resonances in this region were wider and the field H_0 was just in one of such intervals.

To produce the double-side excitation at lower frequencies $\omega \sim 10^6 - 10^8 \mathrm{sec}^{-1}$ the sample may be placed inside an induction coil L (Refs. 48, 49). Including this coil in the tank circuit of a radiofrequency generator, we can use an ordinary nuclear radiospectrometer. When the generator frequency f is measured as the function of the field H (to be more precise when the value $\partial f/\partial H$ is measured, since the measurements are always carried out with the use of the modulation technique), then

$$\frac{\partial f}{\partial H} \sim -\frac{\partial L}{\partial H} \sim -\frac{\partial \delta_{\mathrm{eff}}}{\partial H}, \tag{26}$$

where

$$\delta_{\mathrm{eff}} = \frac{1}{H(0)} \operatorname{Re} \int_0^d H(z)\, \mathrm{d}z \simeq 2 \operatorname{Re} \delta^*. \tag{27}$$

When measuring the dependence of the circuit voltage U on the field, we simultaneously determine the changes of the coil quality factor, i.e. we determine the changes in the quantity of energy S dissipated in the sample: $\partial U/\partial H \sim -\partial S/\partial H$. Determining the surface impedance of the plate in the case

of double-side excitation as $Z=R+iX=(8\pi/c)E(0)/H(0)$ (with an additional factor of 2) and taking into account that $E(0)=-E(d)$, $H(0)=H(d)$, we shall obtain the usual formulae

$$X=\frac{8\pi}{c}\operatorname{Im}\frac{E(0)}{H(0)}=\frac{4\pi\omega}{c^2}\frac{\int_0^d H(z)\,dz}{H(0)}=\frac{4\pi\omega}{c^2}\delta_{\text{eff}}, \tag{28}$$

$$R=\frac{8\pi}{c}\operatorname{Re}\frac{E(0)}{H(0)}=\frac{32\pi^2}{c^2}\frac{S}{|H(0)|^2}. \tag{29}$$

Thus, the measurable values $\partial\delta_{\text{eff}}/\partial H$ and $\partial S/\partial H$ depend on the relation between the fields on the surface $E(0)/H(0)$, i.e. in the long run they depend on the quantity of effective electrons in the skin layer irrespective of the place where these electrons have obtained the energy previously (in the same or in the opposite skin layer). For this reason in the case of the double-side excitation each face of the plate serves simultaneously as the transmitting and receiving one and it is possible to observe all the known radiofrequency size effects.

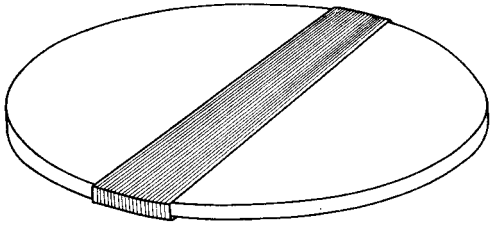

Fig. 6. A sample placed within a measuring coil; double-side excitation.

Fig. 6 illustrates the practically used disposition of the sample relative to the coil turns having a rectangular cross-section. The disposition of this type ensures the plane polarization of an incident electromagnetic wave with vector E applied along the turns. To change the polarization it is necessary to rotate the sample inside the coil. Homogeneity of the H.F. field amplitude on the sample surface is not usually required. If necessary it may be easily obtained by making the coil length exceed the sample size[32,50].

All the results we shall discuss were obtained at low frequencies $\omega\sim 10^7\ \text{sec}^{-1}$ in the case of the double-side excitation. We shall discuss separately effective and ineffective trajectories. Within these two groups the classification of the size effects will be based on the types of the related electron trajectories.

References p. 232

3.2. Closed trajectories

3.2.1. *Cutoff of trajectories*

The records of the quantity $\partial f/\partial H \sim -\partial X/\partial H$ as a function of the magnetic field are shown for bismuth and indium in Figs. 7 and 8*. The conditions of the experiments are outlined in the data given in the captions to the figures. When carrying out the experiments it is sufficient to ascertain that the position of the lines being observed does not depend on the frequency f, but is inversely proportional to the sample thickness. This is the main criterion for the lines of the radiofrequency size effect.

Let us turn first to the lines located on the left part of the records. They correspond to that size effect which was discussed in the previous section [eqs. (21)–(24)]: the size of the extremal electron trajectory is equal to d. Surely the presence of two skin layers does not permit us to conclude that this is a pure cutoff effect. If the field H slightly exceeds H_0, the electron passes through both skin layers and in both layers it behaves as an effective one. This phenomenon is not taken into account in the expressions (21)–(24). But this is, probably, essential for the intensity and shape of the line only. For this reason we shall call this effect the cutoff of the extremal trajectories. When the field H is applied parallel to the surface, the value H_0 is related to the size of the extremal orbit $2p$ in the direction $[\boldsymbol{nH}]$ by the relationship

$$2p = (e/c)\,\mathrm{d}H \tag{30}$$

which is obtained by integration of the corresponding component of eq. (9). By virtue of the non-quadratic dispersion law the extremal trajectory can have a complex form. Then the value $2p$ in (30) is its caliper dimension.

As it is shown in the figures, the cutoff in indium and bismuth is observed in various ranges of the magnetic field. This reflects the difference in calipers of their Fermi surfaces.

Rotating $\boldsymbol{H}$ in the sample plane we change the direction in which the caliper is measured. Using the relation between the line position and the direction of the field, it is possible to determine the form of that part of the Fermi surface which is related to the line. In the bismuth sample, for example, the line in the field H_0 at $\boldsymbol{H} \parallel C_2$ (curve 1 in Fig. 7) is determined by two electron "ellipsoids". When the field is rotated, the "ellipsoids" become nonequivalent and the extremal calipers of orbits on them in the direction $[\boldsymbol{nH}]$ become different (curve 2). (For explanations relative to curve 3 see p. 205).

* All the results for In given below were obtained in experiments carried out by the author together with I. P. Krylov.

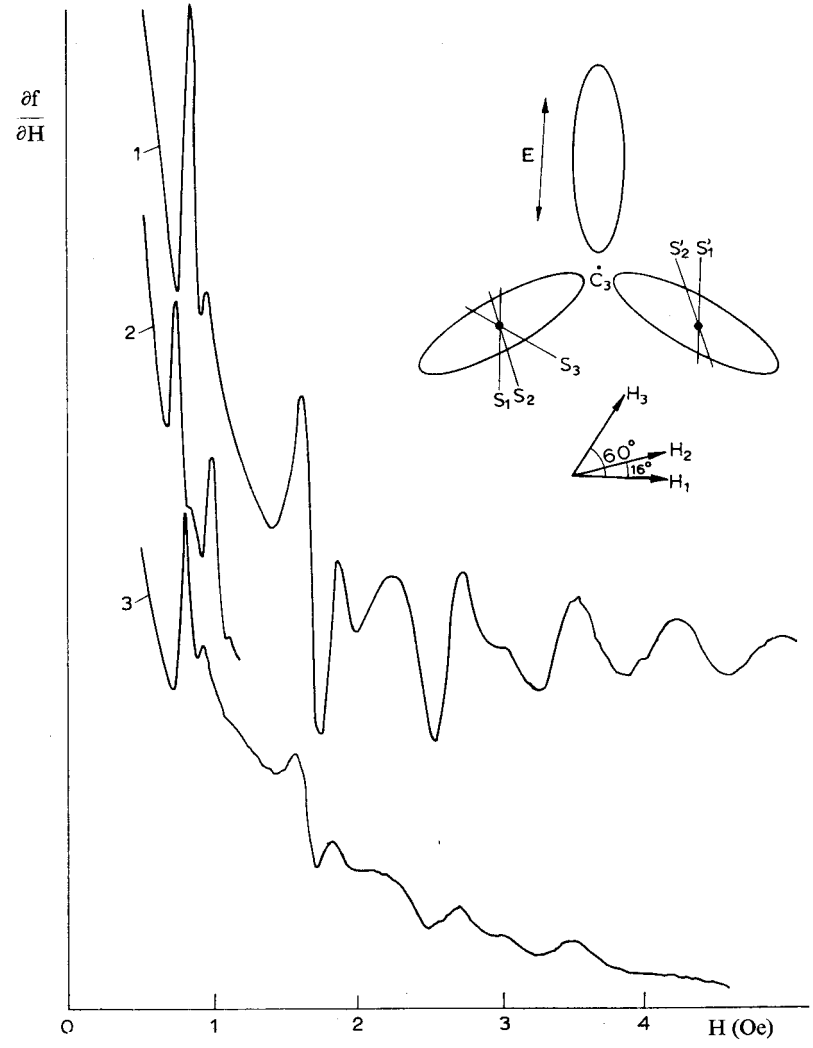

Fig. 7. Records of size effect lines in bismuth for different directions of the magnetic field within the surface plane. $\boldsymbol{n} \| C_3$; the polarization of the electric field is shown at the scheme of the Fermi "ellipsoids" disposition. $d = 1$ mm, $f = 12$ Mc/s, $T = 1.8°$K. Indices at the vectors $\boldsymbol{H}$ and at the extremal cross-sections S and S′ correspond to the number of the curve.

References p. 232

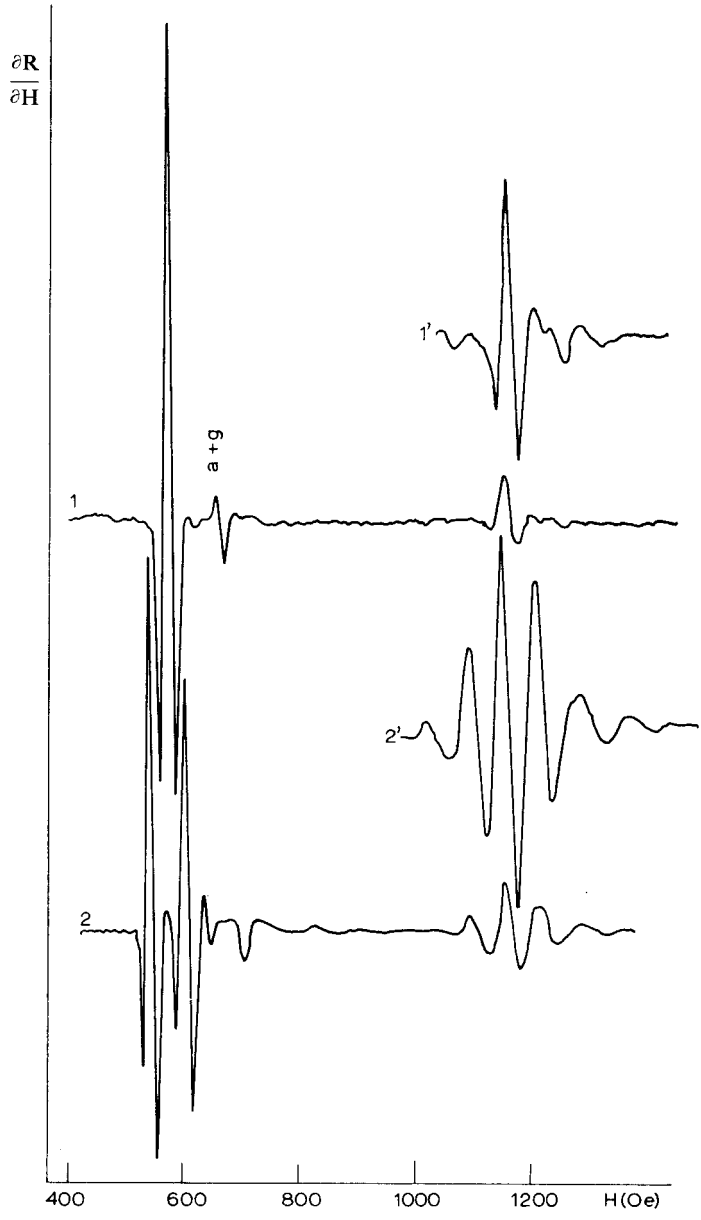

Fig. 8. Records of the size effect lines in indium. $\boldsymbol{n} \| [001]$, $\boldsymbol{E} \| [100]$, $\boldsymbol{H} \| (100)$, $f = 5$ Mc/s, $d = 0.3$ mm. Curve 1: $\boldsymbol{H}$ is parallel to the sample surface. Curve 2: $\boldsymbol{H}$ is inclined at 2°30′. (For explanations relative to curve 2, see p. 212.) Weak lines in double fields are plotted in addition with a magnification of 5 (curves 1′ and 2′). "a + g" denotes a size effect line due to a chain of trajectories (see Ref. 53).

References p. 232

Eq. (30) is obtained with the assumption that H is applied parallel to the plate surface. Under this condition (30) is valid for the Fermi surface of any shape. But we have another situation when the magnetic field is inclined[51]. In the simple case of a spherical Fermi surface, the closed trajectory turns together with the field and always remains within the plane perpendicular to $\boldsymbol{H}$. The field is inclined by an angle φ. The shift of the line relative to the central section may occur, therefore, only due to the change of the effective thickness of the plate (due to the replacement of d with $d/\cos\varphi$).

For a non-spherical Fermi surface, a closed trajectory is not always in the plane perpendicular to $\boldsymbol{H}$. In this case the average drift of the electron along the field during one-half of the period, while travelling from one side of a plane–parallel plate to the other, may differ from zero. When the field $\boldsymbol{H}$ is inclined to the surface, the drift of the electron along the field is projected on the normal to the surface $\boldsymbol{n}$. For this reason, when determining the line position one should take into account the velocity component v_H which is not included in the vector equation (9). In the case, for example, of the Fermi surface in the form of a cylinder with axis $\boldsymbol{P}$ perpendicular to $\boldsymbol{n}$, inclination of the field in the $(\boldsymbol{n}, \boldsymbol{P})$ plane will lead to the line shifting towards the larger fields like $H = H_0/\cos\varphi$. At small values of φ the shift of the line $\Delta H \sim \varphi^2$.

A linear dependence of the shift on the angle is also possible. For example, in the case of the cylinder with axis $\boldsymbol{P}$ inclined to the surface at an angle ψ and with the field in the $(\boldsymbol{n}, \boldsymbol{P})$ plane we have, φ being small,

$$H(\varphi) = H_0 \frac{\cos\psi}{\cos(\psi - \varphi)} \simeq H_0(1 - \varphi \operatorname{tg}\psi). \tag{31}$$

All these formulae are obtained from eq. (9). Their deduction is an excellent exercise for studying the peculiarities of electron motion in the case when the Fermi surface has a complicated shape.

3.2.2. *Chains of trajectories*

Let us return to the field applied parallel to the sample surface. For a complicated Fermi surface several extremal cross-sections and, correspondingly, several cutoff lines may exist for each direction of the field. Sometimes up to seven such extremal sections could be observed in tin[49,52]. These first-order lines should not be confused with the lines in the multiple fields $H_n = nH_0$ $(n = 2, 3, \ldots)$ occurring due to the trajectory chains mentioned above (p. 196). It is such lines that are shown in the right parts of the records in Figs. 7 and 8. These lines are, essentially, another type of size effects caused

by the anomalous penetration of the field and the splashes. As it is shown in the figures, various relations may exist between the amplitudes of the lines of the first ($H=H_0$) and the second ($H=2H_0$) orders. The same phenomenon was observed also in tin[49] and tungsten[44]. The lines in the multiple fields were obtained for one of two groups of first-order lines with approximately the same intensity and were not obtained for another group..

A detailed theoretical analysis of the rate at which the intensity of splashes caused by the chains of extremal trajectories decreases was carried out by Kaner[37]. It was shown that for a system of slowly damping splashes it is necessary that practically all the electrons participating in producing the skin layer current were "focussed" at the same depth, i.e. that they had the same D with an accuracy up to $\Delta D \sim \delta$. We shall illustrate this by some evaluations.

Let the Fermi surface be a sphere with the radius p_0. Near the central cross-section $\partial D/\partial p_H = 0$ and

$$\Delta D \sim D_0 (\Delta p_H / p_0)^2 . \tag{32}$$

This estimate along with the conditions $\Delta D \sim \delta$ determines the relative share of electrons which form the splash. Since the part of electrons in the layer p_H of the Fermi sphere is approximately equal to the areas ratio $p_0 \Delta p_H / p_0^2 = \Delta p_H / p_0$, the intensity of the splash I at the depth D_0 is about $a=(\delta/D)^{\frac{1}{2}}$ of the current value near the surface. The next splash weakens again by a times and therefore the damping becomes very rapid: $I(n) \sim a^n$ [the precise calculations[37] show that an additional factor is introduced into $I(n)$: $I(n) \sim a^n n^{-\frac{3}{4}}$; in the case of $a \ll 1$ this factor is insignificant].

Assume now that the Fermi surface is in the form of a cylinder which is parallel to a metal surface. Then all the electrons have one and the same value D_0 and therefore the current is not spread out in the metal depth ($a=1$). It is shown in Ref. 37 that in this case the splash intensity decreases like $I(n) \sim n^{-\frac{1}{2}}$, i.e. it decreases slowly. In the case of the Fermi surface consisting of a sphere and a cylinder (or even of two cylinders with different radii) both systems of splashes caused by two extremal diameters should decrease in accordance with the exponential law, though with various values of a. The latter phenomenon may be easily illustrated with the aid of the drawings in Fig. 7. As is known, the Fermi surface in bismuth consists of three electron "ellipsoids" (in our case one of them does not contribute to the radiofrequency conductivity because of the polarization of the vector $\boldsymbol{E}$) and a hole-type surface. In the case of field direction $\boldsymbol{H}_1$ (curve 1) formation of the splash system is caused by two electron Fermi surfaces and the resolution of this system is

caused by the hole-type surface. In the case of field direction $\boldsymbol{H}_3$ (curve 3) only one electron "ellipsoid" participates in the formation of the splash system, while the second "ellipsoid" together with the hole-type surface causes the "dissolving" of the splashes. For this reason in the case of the field direction $\boldsymbol{H}_3$ the value a turns out to be smaller and the amplitude of lines decreases more rapidly.

When studying the intensity of the lines of radiofrequency size effect, one should bear in mind that D changes with the number of the line $D(n)=d/n$, and $a^n \simeq (n\delta/d)^{\frac{1}{2}n}$. This leads to the decrease of the difference between the intensity of successive lines of the size effect in multiple fields.

Naturally, in the presence of several extremal diameters the splashes should also occur and at depths of $z_i=\Sigma n_i D_i$. The chain of trajectories, in this case, is composed of various "links". The line of such a chain is shown in Fig. 8 (line "a+g"; cf. Ref. 53).

From the theoretical point of view, the exotic case of the Fermi surface in the form of a cylinder is not the only possibility for the occurrence of weakly damping splashes caused by the chains of the closed trajectories. In Ref. 28 the cyclotron resonance in metals with a non-quadratic spectrum was suggested as the mechanism reducing the contribution of the non-focussed electrons to the conductivity: Ω depends on p_H and therefore only the electrons near the extremal cross-section with Δp_H satisfying (32) participate in the cyclotron resonance. These electrons absorb the energy from the skin layer Ω/v times, while the other electrons are not phased-in with the external field. The experimental observation of such a mechanism of the splash occurrence will entail great difficulties. First of all $\Delta p_H/p_0$ in (32) is of the order of $(\Omega/v)^{-\frac{1}{2}}$ and therefore the expression (32) takes the form $\Omega/v \gg D_0/\delta \gg 1$. It means that very long free paths, strong magnetic fields and high frequencies are required. Then, in the case of a plane–parallel plate the following two conditions are superposed simultaneously on the field $H: \omega = n\Omega$ and $D=d/n'$ (n and n' are integers). The scheme of a proper experiment would therefore become considerably complicated.

Another way of decreasing the splash damping, which may be used for any relationship between ω and Ω, consists in a slight inclination of the field relative to the surface[37].

Let us turn again to the spherical model of the Fermi surface. If the field is inclined to the surface at an angle φ, only those electrons repeatedly return to the skin layer which have sufficiently small average velocity of drift along the field v_H. The corresponding orbits are near the central closed orbit in the interval $\Delta p_H/p_0 \sim \delta/l\varphi$. Assuming that all these effective electrons are focussed

References p. 232

at a depth D_0 in the interval $\Delta D \ll \delta$, and using the expression (32) we obtain the following condition for φ:

$$\varphi^2 \gg \delta D_0 / l^2 . \tag{33}$$

On the other hand, to ensure the slow damping of splashes it is necessary that these electrons make the main contribution $(\Delta p_H \cdot p_0)(l/D_0) \gg p_0^2$, i.e.

$$\varphi \ll \delta / D_0 . \tag{34}$$

It follows from (33) and (34) that when

$$D_0^3 \ll l^2 \delta , \tag{35}$$

there is a range of inclinations of the magnetic field at which the skin current is determined mainly by electrons near the central section focussed at a depth D_0. Under these conditions the splashes damp slowly: $I(n) \sim n^{-\frac{1}{2}}$. The condition (35) is sufficiently rigid and, besides, as in the case of a cylinder, one and only one extremal diameter is required. Therefore, strictly speaking, the effect of the considerable decrease of the splash damping at the inclined magnetic field suggested in Ref. 37 is not checked experimentally. For indium and tin, however, in a number of cases the increase of the line intensity in multiple fields was observed for inclined fields, in spite of the fact that the experimental conditions corresponded to the relation $D_0^3 \simeq \delta l^2$ instead of the expression (35). In a sample of tin, for example, with $d = 0.5$ mm and $\boldsymbol{n} \parallel [001]$, the intensity of a line with $H_0 \simeq 400$ Oe (line 1_3, see Ref. 52) decreased by a factor of 20 after transition to the double field. At an inclination of 3° the line amplitude in the field $2H_0$ increased by a factor of 2 while the main line remained unchanged.

3.3. Helical trajectories

3.3.1. *Vicinity of limiting point*

While the field $\boldsymbol{H}$ and, hence, the mean velocity $\overline{\boldsymbol{v}_H}$ are parallel to the surface, the behaviour of helical trajectories is the same as that of the closed trajectories (see Fig. 9). Assume, for example, that due to the complicated dispersion law we have a non-central orbit with $\overline{v_H} = 0$ and the extremal caliper in the $[\boldsymbol{nH}]$ direction. The line of the size effect caused by such an orbit will not differ from the lines caused by the central orbits (closed trajectories).

Incline, then, the magnetic field at an angle φ. This leads immediately to the appearance of the projection $\overline{\boldsymbol{v}_H}$ directed along the normal and as a result the depth of the effective points changes. A system of weakly damping

splashes may also occur under such conditions. These splashes are formed owing to the electron trajectories passing directly from the surface. Let us discuss this problem in detail first for the case of helical trajectories in the vicinity of an elliptical limiting point in the field H inclined to the surface at a small angle.

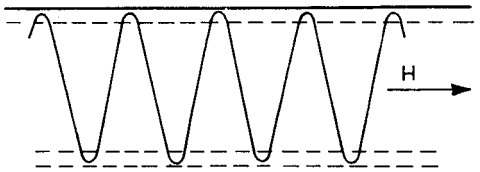

Fig. 9. A helical trajectory in a magnetic field parallel to the sample surface.

In first approximation, all electrons in this vicinity drift equally along the field during the period $T_0 = 2\pi/\Omega$. This phenomenon is well known in electron optics as "focussing of electrons by a longitudinal magnetic field". At the limiting point, the velocity $\boldsymbol{v}_0$ is parallel to $\boldsymbol{H}$, $|v_z| = v_0 \sin \varphi$, $mv_0 = K^{-\frac{1}{2}}$ (K is the Gaussian curvature of the Fermi surface, $\varepsilon(p) = \varepsilon_F$ at the limiting point). As the average drift of an electron into the interior of the metal during the period T_0 is equal to $u_{\text{lim}} = |v_z T_0| = 2\pi c m \bar{v}_z / eH$, then

$$u_{\text{lim}} = \frac{2\pi c}{eH} K^{-\frac{1}{2}} \sin \varphi . \tag{36}$$

In the case of a spherical limiting point $K^{-\frac{1}{2}} = p_0$, i.e. it is equal to the radius of the Fermi sphere, and

$$u_{\text{lim}} = \pi D_0 \sin \varphi , \tag{37}$$

where $D_0 = 2p_0 c/eH$. Of course the focussing takes place repeatedly after one, two, three or more revolutions in the electron trajectories.

Let us now deduce the conditions which should be imposed upon the angle φ of the magnetic field inclination to ensure the occurrence of slowly damping splashes of the field deep in the metal. The first condition is quite obvious: $u_{\text{lim}} \gg \delta$. It means that the splash should leave the skin layer. This condition leads to the following inequality

$$\varphi \gg \delta / v_0 T_0 . \tag{38}$$

The second condition may be formulated in the following way: among the focussing electrons there should be effective ones. The angular interval on the Fermi surface between the limiting point and the effective region is equal

to φ (see Figs. 3 and 10). Consequently the angular size ψ of the region occupied on the Fermi surface by focussing electrons should exceed φ, i.e. $\psi > \varphi$. The magnitude ψ is evaluated in the following way: for the deepest splashes which may be reached by electrons directly from the surface ($z \sim l \sin \varphi \sim l\varphi$), the dispersion of the displacement Δu should be less than δ.

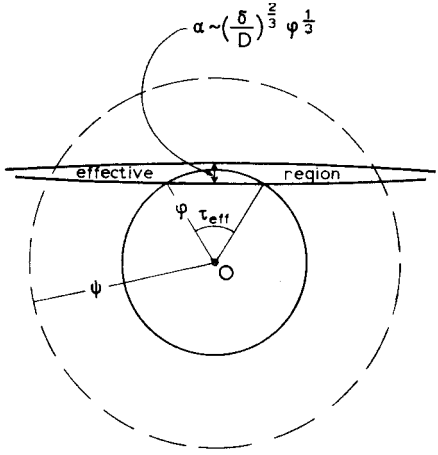

Fig. 10. Vicinity of the limiting point O at a Fermi sphere in an inclined magnetic field.

Since the electron velocity along the field is $v_H \sim v_0(1 - \frac{1}{2}\psi^2)$, we shall obtain $l\varphi\psi^2 \sim \delta$, hence $\psi \sim (\delta/l\varphi)^{\frac{1}{2}}$ and

$$\varphi \ll (\delta/l)^{\frac{1}{3}}. \tag{39}$$

The conditions (38) and (39) determine the interval of angles φ at which the group of effective electrons will be successively focussed at depths $u_n = nu_{\text{lim}}$ ($n = 1, 2, \ldots$). It should be emphasized that the constant a which determines the significance of this group from the viewpoint of contribution to the skin current enters only once into the expression for the amplitude, irrespective of the splash number. The decrease of the amplitude during the transition from n-splash to $(n+1)$-splash is determined only be the length of path $A_n \sim a \exp(-u_n/l\varphi)$. That is why the focussing at a depth of distant splashes was required in (39). Violation of (39) means that the limiting point is far from the effective region. It has been shown in Ref. 54 that splashes do exist in this case too, but the electrons which form such splashes do not belong to the vicinity of the limiting point. (About forming the splashes when $\varphi \gg (\delta/l)^{\frac{1}{3}}$, see Section 3.3.3.)

References p. 232

An example of the size effect from the limiting point is shown in Fig. 11. This effect may be easily distinguished as the period ΔH greatly depends on the inclination angle

$$\Delta H = \frac{2\pi c}{eH} K^{-\frac{1}{2}} \varphi . \tag{40}$$

The existence of a line at a certain magnetic field means that the trajectories in the vicinity of the limiting point contain integer revolutions between the surfaces of the plate at this field. It should be noted, that transition from one size effect line to the other is related to the change of the field while the length of the trajectory from one surface of the plate to the other remains unchanged. When passing from one number to the other the amplitude decreases due to the dependence $a(H)$, as well as due to the change of the absolute value of the line width H. The latter is essential for the measurements of a derivative.

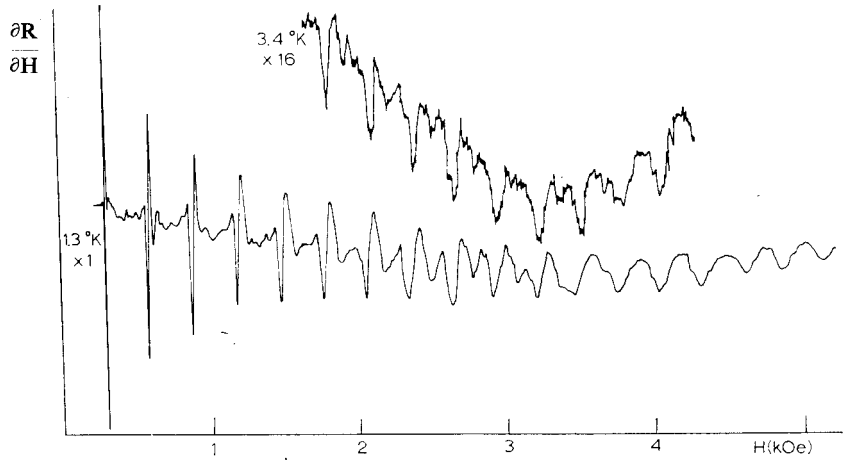

Fig. 11. Records of the limiting point size effect lines in indium. The point is near [111]. $\boldsymbol{n} \parallel [011]$, $\boldsymbol{E} \parallel [111]$, $d = 0.3$ mm, $\varphi = 7°15'$, $f = 1.6$ Mc/s.

As it is shown in Fig. 11, the temperature increase, i.e. the decrease of the length of path l, influences only the amplitude of the lines but not the line width. This phenomenon may be easily understood if we try to retrace how the same result follows from the theory [eqs. (11)–(19)].

Remember that the sharp inhomogeneity of the field in the skin layer can

be described with the aid of a superposition of monochromatic plane waves whose wave numbers k have a continuous spectrum of width $\Delta k \sim \delta^{-1}$. The electrons drifting inside the metal interact most effectively with those field-spectrum harmonics whose wavelength λ is contained an integer number of times in the distance u_{lim}: $u_{\text{lim}} = N\lambda$. This condition separates from the continuous spectrum a discrete series of wavelengths which can penetrate to an anomalously large depth into the metal. The interference of these waves gives rise to quasi-periodic field maxima at depths $z_n = nu_{\text{lim}}$. The widths of these maxima are determined by the width of the initial wavelength spectrum and therefore they are of the order of δ. The height of the maxima and their decrease with distance are determined by non monochromaticity of the waves with anomalous deep penetration, i.e. in final analysis by the length of the electron free path l.

3.3.2. *Extremal non-central orbits*

As was stated above, in the case of a complicated dispersion law the extremal non-central orbits may exist. Let us consider the behaviour of the size effect lines caused by such orbits in an inclined field[51]. It is necessary, of course, to account again for the drift of electrons along the field. The lines are observed when $d = u$, where $u = \Omega^{-1} \int_{\tau_1}^{\tau_2} v_z \, d\tau$ and τ_1 and τ_2 are two effective points of the orbit. When the pitch of the helical line is $h \ll D$ ($h = v_H T_0 = 2\pi \overline{v_H}/\Omega$), we have the following approximate formula for u

$$u_{n-\frac{1}{2}} = D \cos \varphi + (n - \tfrac{1}{2}) h \sin \varphi, \qquad (n = 0, 1, 2, \ldots). \tag{41}$$

The factor $(n - \frac{1}{2})$ is equal to a number of revolutions in electron paths from one surface of the plate to the other. The value $n = 0$ corresponds to the case where the component of the drift velocity $v_H \sin \varphi$ is opposite to the main motion along the turn and its projection on the z axis is negative. The values $n = 1, 2, \ldots$ correspond to the positive projections of the velocity (see Fig. 12, where a helical trajectory is once more pictured in the lateral projection). Using (41) at small values of φ, we obtain for the line position

$$H_{n-\frac{1}{2}} = H_0 \left[1 + (n - \tfrac{1}{2}) \frac{h}{D} \varphi \right], \qquad (n = 0, 1, 2, \ldots). \tag{42}$$

It is clear from the meaning of the factor $(n - \frac{1}{2})$ that the amplitudes of the first two lines should be of the same order, while the others should decrease rapidly with number due to the increase of the path Λ from one surface to the other.

Thus, the size effect lines caused by the non-central orbits should split as

the field inclines. Such a splitting was experimentally observed in indium[51] (see Fig. 8; under favorable circumstances the line corresponding to $n+2$ is seen also; on the curve of Fig. 8 it is obscured by the line "a+g"). The splitting would exceed the line width only if $h\varphi \gg \delta$, i.e. v_H should be sufficiently large. This condition is satisfied in indium due to the form of its Fermi surface.

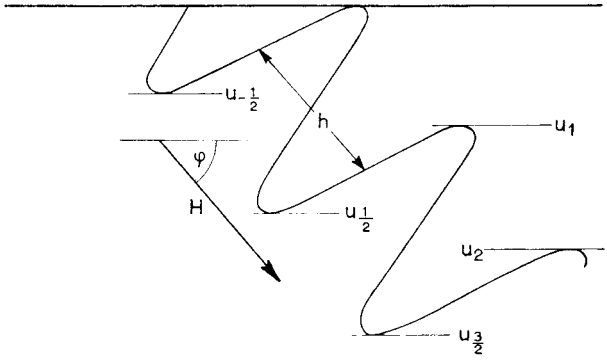

Fig. 12. A helical trajectory in an inclined magnetic field with two effective points through a period.

As always, the radiofrequency size effect may be brought in correspondence with a picture of splashes inside a metal. The helical trajectory, shown in Fig. 9, contributed to both the skin current and to the splash at a depth D. When the condition $h\varphi \gg \delta$ becomes satisfied, the splashes $u_n = hn \sin \varphi$ $(n=1, 2, \ldots)$ split from the skin layer and a set of splashes $u_{n-\frac{1}{2}}$ determined by the formula (41) occurs instead of the splash at a depth $u=D$. The splash amplitude will certainly decrease with the increase of the index along the exponential curve

$$A_k \sim a \exp(-\Lambda_k/l),$$

where

$$\Lambda_k \sim k\pi D, \qquad (k = \tfrac{1}{2}, 1, \tfrac{3}{2}, \ldots)$$

and the factor a, as previously, determines the contribution to the skin current made by the focussing electrons. Generally speaking, each of these splashes may be initial for a chain and the damping along the chain will be determined by the factor a^n. When the exponential factor in A_k extinguishes all splashes but $u_{\pm\frac{1}{2}}$, then the size effect line in the double field will split into 3, the triple field into 4, etc. (see Fig. 8).

References p. 232

3.3.3. *The spherical Fermi surface in an inclined magnetic field*

In an inclined field, two functions D and h depending on p_H are contained in the expression for u. In the case of indium, the extremum $u(p_H)$ is determined by the extremum $D(p_H)$. However, this is not necessary. The function $u(p_H)$ may have an extremum when $D(p_H)$ and $h(p_H)$ are not extremal if taken separately. In particular this is true for the spherical Fermi surface.

Let us determine the orbit position on the sphere with the aid of an angle θ (see Fig. 13). The value $\theta=0$ corresponds to the central orbit and $\theta=\pm\frac{1}{2}$ corresponds to the limiting points. Effective points exist in orbits at $|\theta| \leq \theta_{max}$, where $\theta_{max}=\frac{1}{2}\pi-\varphi$; at $\theta=\theta_{max}$ the trajectory has only one effective point through a period (see Fig. 3).

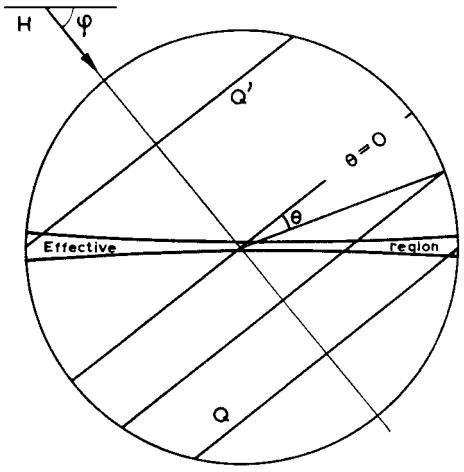

Fig. 13. Different orbits on the Fermi sphere in an inclined magnetic field.

In the previous description of the slowly damping splashes caused by the closed trajectories it was assumed that $l \gg D$. It gave us the possibility to formulate conditions (34) and (35) under which the contribution to the skin current made by the helical trajectories could be neglected. Let us now consider another case: conditions (34) and (35) are not satisfied. Then all the orbits within the range $(-\theta_{max}, \theta_{max})$ are equivalent. Their contribution to the skin current is proportional to a number of electrons contained in them.

In Fig. 12 a trajectory with $\theta \neq \theta_{max}$ is shown. Sphericity of the Fermi surface permits us to write instead of (41) precise formulae for $u_n(\theta)$ and

$u_{n-\frac{1}{2}}(\theta)$

$$u_n(\theta) = n\pi D_0 \sin\varphi \sin\theta,$$
$$u_{n-\frac{1}{2}}(\theta) = D_0 \cos\varphi \cos\theta\,(\pi n q + \sqrt{1-q^2} - q \arccos q), \quad (n = 0, 1, 2, \ldots), \tag{43}$$

where

$$q(\theta) = \operatorname{tg}\varphi \operatorname{tg}\theta, \qquad q(\theta_{\max}) = 1. \tag{44}$$

The effective points u_n cannot be observed in the size effects of the first order since $u_n < u_{n-\frac{1}{2}}$. Let us turn to the effective points with half-integer indices considering $u_{n-\frac{1}{2}}$ as functions of the angle θ. It can be easily shown that $u_{-\frac{1}{2}}$ (the depth of the effective points for the orbits with $\theta<0$) is a monotonic function of θ; the functions $u_{n-\frac{1}{2}}$ with $n>0$, which have a physical sense for the values $\theta>0$, may have extrema. For example, the function $u_{\frac{1}{2}}$ has two extrema with positions determined by the equation

$$\pi - Cq\sqrt{1-q^2} = \arccos q, \qquad C = \operatorname{tg}^{-2}\varphi. \tag{45}$$

One of them is a minimum which is very shallow for all values of φ. Another is a maximum located in the region $q<1/\sqrt{2}$. It may exceed $u_{\frac{1}{2}}(0)$ by more than 20% (see Fig. 14).

Existence of an extremum of $u(\theta)$ means that focussing of a group of effective electrons takes place at the depth u_{ext}. Hence a splash must arise at that depth, and when $d=u_{\text{ext}}$ a size effect must also occur.

We consider first $u=u_{\max}$. It appears to be a quite peculiar situation. When the conditions (33)–(35) are satisfied, the conductivity is determined mainly by the vicinity of the central orbit. However, when H decreases [i.e. when D_0 increases and the condition (35) ceases to be fulfilled], another splash should appear and this splash should be followed by the appearance of the second size effect line satisfying the condition $d=u_{\max}$. Possibly, just such a structure of the H.F. field within a metal explains the splitting of the lines of the cyclotron resonance in sodium in the presence of an inclined magnetic field[55], though the splitting in this case occurs at much smaller tip angles than those which may be expected on the basis of the simple calculations given above.

The magnitude $u_{\min}$ practically does not differ from

$$u_\varphi = \tfrac{1}{2}\pi D_0 \sin 2\varphi, \tag{46}$$

where the effective point of the boundary effective trajectory with $\theta=\theta_{\max}$ is

References p. 232

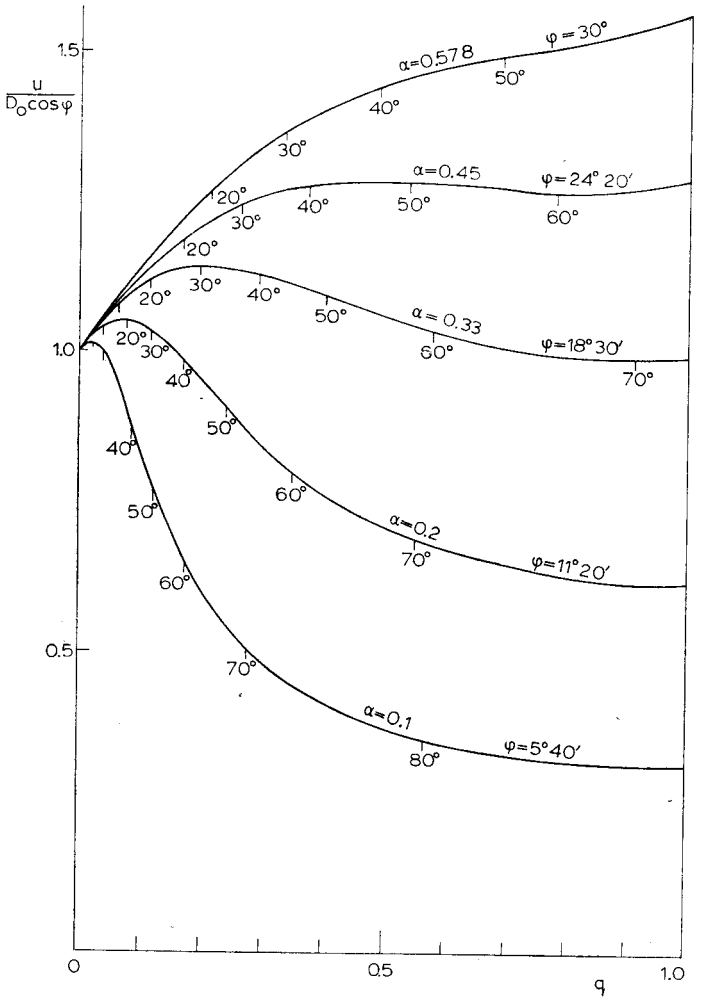

Fig. 14. Graphs which illustrate eq. (43) for $u_{\natural}$ $(n = 1)$; $\alpha = \operatorname{tg} \varphi$.

located. It follows from the comparison of (46) and (37) that if the field is inclined the limiting point splashes convert into the boundary effective trajectory splashes at the depth nu_{φ} $(n=1, 2, \ldots)$. Subsequent inclination of the field leads to the decrease of the difference $u_{\max} - u_{\min}$ (see Fig. 14). At $\varphi \sim 20$–25 ° the splashes (and corresponding size effect lines) should amalgate. Their intensity under these circumstances should increase because a focussing of a comparatively wide layer of orbits takes place. A further increase

of the angle φ results in deterioration of the focussing and the size effects lines should disappear.

3.4. Open trajectories

In the case of open trajectories, the most essential is the direction of the field relative to the crystallographic axes, but not relative to the metal surface, since it may occur that the open trajectories exist only in a small range of angles. When the average electron velocity $\bar{\boldsymbol{v}}$ is directed along the surface, the effect does not differ from that of the closed trajectories. The line position determines the extremal "amplitude of crimping" of the open trajectories. If the angle γ between $\bar{\boldsymbol{v}}$ and $\boldsymbol{n}$ differs from 90°, we have an analogy with the helical trajectories. The pictures shown in Figs. 3, 9 and 12 may be used for a schematic illustration of the behaviour of the open trajectories if $\boldsymbol{H}$ is assumed to be perpendicular to the picture plane (and $\gamma=\frac{1}{2}\pi-\varphi$). At small values of γ, when the "crimp" of the trajectory is insignificant, or, to be more precise, when we have only one effective point during the period, as it is shown in Fig. 3, the value u of the average drift of electrons inside the metal is the same for all open trajectories and is given by

$$u = (cb/eH)\cos\gamma, \tag{47}$$

where b is the period of the open orbit (reciprocal lattice). Thus, the "focussing" in this case is effected automatically due to the dispersion law. The requirement for the presence of effective electrons among the focussing ones means that trajectories having at least one effective point should be contained among the open trajectories (concerning the opposite case, see p. 219).

The size effect from the open trajectories was observed in tin only[38]. To save space we shall not demonstrate here the curves which are given in the original paper. We only note that at $\gamma=0$ (which is the condition of the experiment) the velocity $\boldsymbol{v}$ in the effective points should be perpendicular to the mean velocity $\bar{\boldsymbol{v}}$.

3.5. Trajectories with breaks

It seems that we have already discussed all possible types of electron orbits. However, when the size effect in indium was studied[53], a number of "superfluous" lines was observed (the indium Fermi surface had already been known approximately from both experimental and theoretical investigations). None of the mechanisms discussed above could explain the existence of these "superfluous" lines. The detailed study of the anisotropy of these lines, their behaviour at an inclination as well as the form of the Fermi surface as a whole

made it possible to show that the occurrence of these lines was caused by the presence of breaks in the electron trajectories. The example of an orbit with breaks existing in indium is shown in Fig. 15.

The occurrence of size effect lines caused by breaks in the electron trajectories indicates the presence of an electromagnetic field not only near the splashes, but also in the intervals between them. To estimate qualitatively

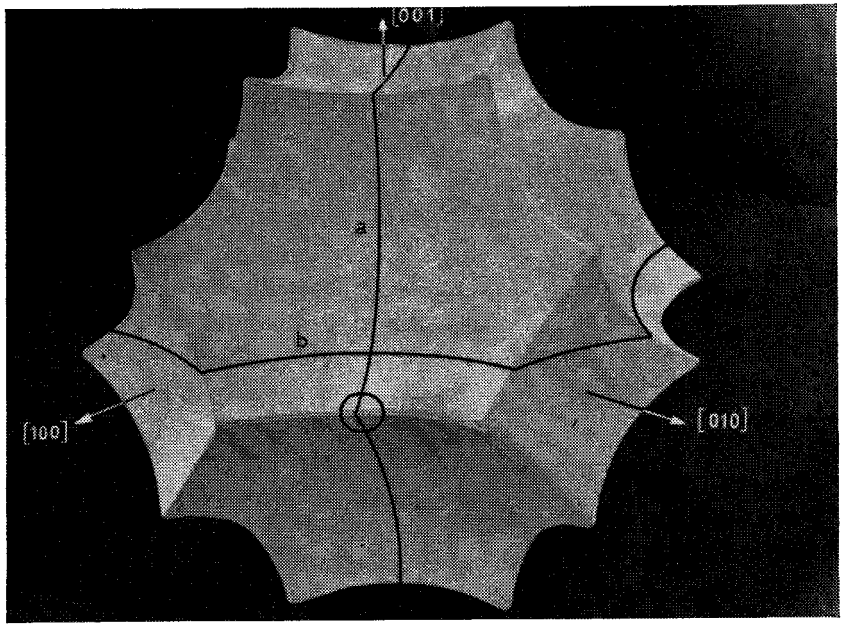

Fig. 15. Fermi surface of indium in the second zone in accordance with the nearly-free-electron model. Circled part of the orbit *a* denotes a break; *b* is a non-central orbit with an extremal caliper in [100] direction.

this field let us consider the distribution of the electromagnetic field in the depth of a metal with a Fermi surface in the form of a circular cylinder. An electron, which obtained the addition to the velocity Δv in the skin layer, passes into a depth along the circular trajectory. If at a depth z this electron moves at an angle κ to the surface, the horizontal component of the current produced by this electron is equal to $e\,\Delta v \cos \kappa$. (The vertical component is compensated by the electrons moving towards the surface along the analogous trajectory at an angle $\kappa_1 = 2\pi - \kappa$.) Taking into account the fact that the number of electrons belonging to the given trajectory at a depth z is

proportional to $1/\sin\kappa$, we obtain the current produced by these electrons at $z \gg \delta$ and $D-z \gg \delta$, i.e. far from splashes, equal to

$$j(z) \sim j(0)\sqrt{\delta/D}\,\operatorname{cotg}\kappa. \tag{48}$$

Let us assume now that the trajectory has a break, i.e. the condition $D \gg \delta$ is still valid but at the same time within some part of the trajectory at a distance $\Delta z \lesssim \delta$, the change of the angle κ is $\Delta\kappa \sim \kappa$. It is clear that in this case the jump of the function $j(z)$ will also occur at a distance $\Delta z \lesssim \delta$.

3.6. Trajectories of ineffective electrons

Let us consider first the magnetic field directed along the normal to the surface[56]. The closed, helical and open effective trajectories with the effective points located at various depths are certainly possible in the case of a non-spherical Fermi surface in the field perpendicular to the metal surface. These possibilities occur due to the drift of electrons along the field [the component $v_H(\tau)$] which is absent in eq. (9). Naturally, the radiofrequency size effects similar to those which were discussed above should occur on these trajectories. The size effects of such a type were not yet observed experimentally, though there were works devoted to the study of the cyclotron resonance for such orbits[57, 58].

However, there may be no such effective trajectories in a metal. For a spherical Fermi surface, for example, the region of effective orbits, shown in Fig. 13, constricts into a strip whose width has an angular size $\theta \sim \delta/l$, as in a zero field. The whole free path of these effective electrons is within the skin layer. The electrons which penetrate into the metal are moving along the helical trajectories at an angle β to the field. The ineffective electrons in a zero magnetic field determine the small but deeply penetrating component of the field which damps as $e^{-\xi}/\xi^2$, where $\xi = z/l$. In the presence of a field, an ineffective electron also carries information concerning the instantaneous value of the skin layer electric field into the interior. However, as its velocity component $v_\perp = (v_x^2 + v_y^2)^{\frac{1}{2}}$ perpendicular to $\boldsymbol{H}$ rotates in the plane (x, y), the field component $e^{-\xi}/\xi^2$ converts into a helical one [we would remind the reader that the conditions (1), (8) and (20) are assumed to be satisfied]. The translation period of this helix may depend only on the extremal values $\overline{v_z} T_0(p_H)$, such, for example, as values $v_z T_0$ in the vicinity of the limiting point. Thus, refusing the requirement for the electron effectiveness, we obtain a harmonic distribution of the field inside a metal instead of splashes and, respectively, a sinusoidal component in the plate impedance instead of narrow size effect lines (see Fig. 16).

References p. 232

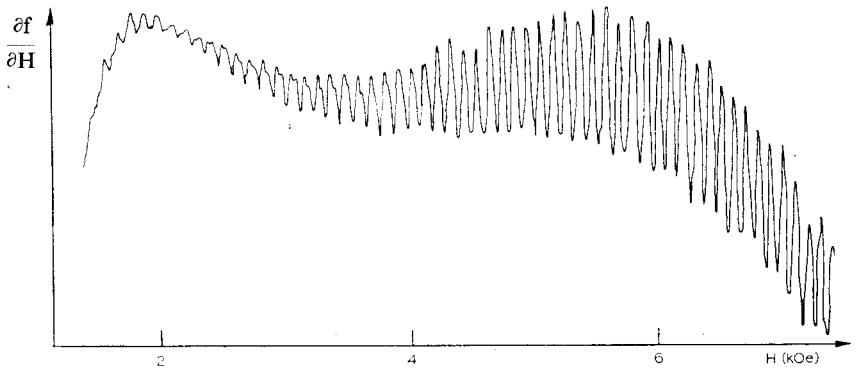

Fig. 16. Record of a size effect related to ineffective electrons in tin[56]. $\boldsymbol{n} \parallel [100]$, $\boldsymbol{E} \parallel [010]$, $d = 0.96$ mm, $f = 5.2$ Mc/s, $\sphericalangle(\boldsymbol{n}, \boldsymbol{H}) = 17°$.

Such a radiofrequency size effect at the normal field has been observed in tin only. As it was mentioned in Ref. 56, there are a number of obscurities in the experimental results. We wil not dwell upon them here.

For the magnetic field directed along the surface a similar effect exists owing to electrons in open orbits[59]. If the corresponding trajectories have $\overline{v_z^{\P}} \neq 0$, but at the same time have no effective points, again a sinusoidal component in the impedance appears instead of sharp size effect lines. Such an effect was detected in cadmium[59].

3.7. Conclusion

Here at the end of this section we present Table 1 summarizing all known size effects in the anomalous skin condition.

The following remarks should be made about Table 1.

1) We have discussed the experiments with a plane–parallel plate only. In principle the radiofrequency size effects may occur in samples of other form too. No work dealing with such samples was done up till now.

2) Azbel[60] noted that in principle observation of the cutoff of the quantum oscillations in the high-frequency surface impedance is possible. A peculiar mixing of quantum and quasi-classical effects takes place in this case: the quantum oscillations may be observed only when the corresponding trajectory fits inside the plate. Since the quantum oscillations appear usually only in fields of several kilooersteds, the single-crystal plane–parallel films with a thickness of about 10^{-4} cm are required for observation of such cutoff effects. That is hardly feasible now.

References p. 232

TABLE 1

Cutoff of cyclotron resonances[35]	Anomalous penetration	Cutoff	Effective electrons
Cutoff of non-resonant orbits at high frequencies ($\omega \sim \Omega$)[34,47]			
Cutoff of non-resonant orbits at low frequencies ($\omega \ll \Omega$)[32,48,49,58]			
Chain of trajectories caused by the extremal orbits[36,44]		Mean velocity $\bar{v}_z = 0$	
Weak damping: at cyclotron resonance[28]			
Weak damping: at cylindrical Fermi surface[36]			
Weak damping: at inclined magnetic field[37]			
Extremal helical trajectories[51]		$\bar{v}_z \neq 0$	
Vicinity of limiting points[38,62]			
Open trajectories with effective points[38]			
Breaks of electron trajectories[53]			
Ineffective trajectories at $\boldsymbol{H} \parallel \boldsymbol{n}$[56]		$\bar{v}_z \neq 0$	Ineffective electrons
Open ineffective trajectories[59]			

4. Shape of line and various experimental factors

In the previous section we discussed various cases of occurrence of size effects and the position of the line in the scale of magnetic fields. These problems may be considered to some extent as a first approximation in the solution of the size effect problem. The next approach from this viewpoint consists of the solution to the problem of the line shape.

In most of the theoretical works use is made of the first approximation only. The solution of (18) is not simple but feasible, since one of the four integrations concerned is trivial as $\partial f_0/\partial\varepsilon$ may be considered as a δ-function and integration over τ and τ_0 may be done with the use of the stationary phase method. However, in the course of transformation (19) from the Fourier representation to the distribution of the field inside a metal, the calculations become so complicated that it is necessary to introduce some simplifications in which the shape of the line is practically dropped out.

Thus, the problem of the line shape is considerably less studied than those problems discussed above. For this reason, the material presented in this section may be considered possibly as a statement of the problem only. We will limit ourselves to a brief description of all the known experimental factors influencing the line shape.

1) *Mode of excitation.* Undoubtedly the line shape of the size effects should

greatly depend on whether the excitation of the electromagnetic field in the plate is of one- or double-side type (see pp. 197–200 above). At present, however, the experiments in which various modes of excitation are directly compared with one another are not yet known. All experimental results used below belong to the case of double-side excitation.

2) *The relation between the resistance R and the reactance X.* Since the position of the line in the size effect is independent of the frequency ω, the functions $R(H)$ and $X(H)$ are not interrelated through differential expressions arising from the Kramers–Kronig relations as in the case of resonance effects. It seems, therefore, that there is no reason to expect the line shape to depend on what function is being studied in the case (the function $\partial R/\partial H$ or the function $\partial X/\partial H$). The experiment carried out by Krylov[61] showed, however, that such a dependence really existed. In all the experiments the extrema of the function $\partial R/\partial H$ within the line width always correspond to the places of the greatest changes of the function $\partial X/\partial H$ and vice versa. Thus, the qualitative relations between ΔR and ΔX are the same as those, for example, observed within the lines of the nuclear resonance. A good quantitative agreement is observed in some cases too[61]. There is, therefore, a basis to assume that the observed relation between ΔR and ΔX in the size effect may be caused by some common properties of the equations for the high-frequency current distribution in the metal.

3) *Type of size effect and the dispersion law.* Under similar conditions the line shape varies of course for the size effects of various types (cf., for example Figs. 8 and 11). The line shape of the limiting point size effect is well reproduced for various limiting points even in different metals. In the case of the cutoff of the closed trajectories it is quite different for different extremal orbits. This is obviously related to the behaviour of the dispersion law in the vicinity of the extremal cross-section. It is possible to put forward the following two obvious influencing mechanisms of the dispersion law. First, the line shape may depend on the character of the extremum of the function $D(p_H)$: the measurable caliper may reach a minimum or a maximum on the extremal orbit (see Fig. 17). Second, the shape of the line should depend on the shape of the extremal trajectory in the skin layer, i.e. it should depend on the length of the electron drift in the skin layer $\sqrt{(R\delta)}$ related to the value δ (R is the radius of the trajectory curvature at the effective point). Presumably the influence of the trajectory form is more important.

Let us illustrate this by an example. From the topological viewpoint the

Fermi surface of tin in the fourth zone consists of two planes connected by "tubes". According to the experimental data[35, 47, 49], their deviation from a cylinder does not exceed several per cent and D reaches the maximum at the central cross-section; the central cross-section of the tube practically does not differ from a square. When the magnetic field is applied along the cylinder

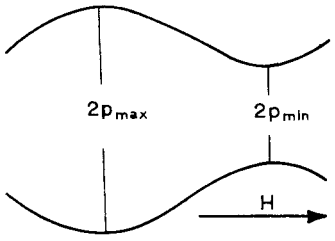

Fig. 17. Different types of the extremal calipers at Fermi surfaces.

axis (crystallographic axis C_4), the central cross-section of the cylinder causes a square closed trajectory. Depending on the orientation of the normal $\boldsymbol{n}$, either side or diagonal of this square may be parallel to the sample surface. In the latter case the trajectory enters the skin layer at an angle. The shape of the line is different in these two cases (see Ref. 49, curves 1_1 and 1_2).

4) *Frequency*. When choosing the frequency ω it is necessary to satisfy the quasi-static condition (20) to exclude the influence of the relation between Ω and ω upon the shape of the line. The frequency in this case may influence the shape of the line only through the depth of the skin layer, through the ratio δ/d. The dependence of the line width on the frequency in bismuth is shown in Fig. 18 (the same line as that on curve 1 in Fig. 7). It follows from Fig. 18 that the relative width of the line Δ_H/H_0 is fully determined by the value δ/d, at least at $f \sim 3$ Mc/s (generally speaking, at the maximum frequency studied one can expect an influence of the non-uniformity in the sample thickness). The line presumably stretches to the right of H_0 up to those values of the field at which the electron trajectory still can brush against both skin layers. Using the distance between two minima as Δ_H, we shall see that at $f \sim 3$ Mc/s, $\Delta_H/H_0 \sim 2\,\delta/d = 0.25$ and hence $\delta \sim 10^{-2}$ cm. At the same time, if we recalculate the result of the measurements of the real part of the impedance at high frequencies with the use of formulae (4), we shall obtain $\delta \sim 10^{-3}$ cm. Discrepances of the same sign were observed in indium-62 and tin also. These discrepances are obviously related to the non-exponential distribution of the field within the skin layer[5, 18, 20]: the field considerably

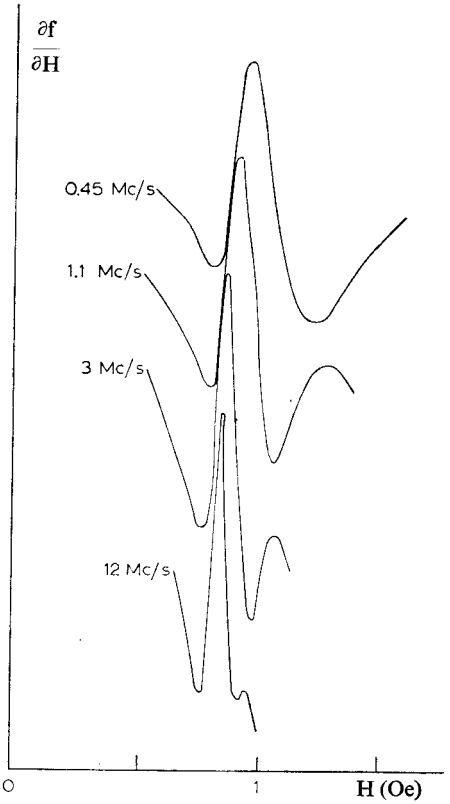

Fig. 18. The dependence of the width of the size effect line in bismuth on the frequency. The experimental conditions are the same as for the record in Fig. 7, curve 1.

differs from zero at distances exceeding the value δ_{eff}, evaluated from the impedance with the aid of eq. (28).

5) *Sample thickness.* The possible range of thickness values is determined by the inequalities (1). Practically, however, this range is not fully used due to experimental difficulties which increase rapidly as the sample thickness decreases. Thus, for example, at $d=10^{-2}$ cm it is very difficult to obtain a plane–parallel plate, i.e. to obtain the same d along the whole sample with an accuracy of at least several per cent. It is interesting that for a wedge shaped sample the size effect line does not smear out but splits: two lines corresponding to $d_{\min}$ and $d_{\max}$ appear instead of one line (see Fig. 19). The position of the limiting point size effect line greatly depends on the angle φ [see eq. (40)]. For this reason these lines may split also due to bending of the

sample; such a split was observed experimentally in indium. For samples that are free of such defects, the shape of the line does not depend on d if the latter satisfies (1).

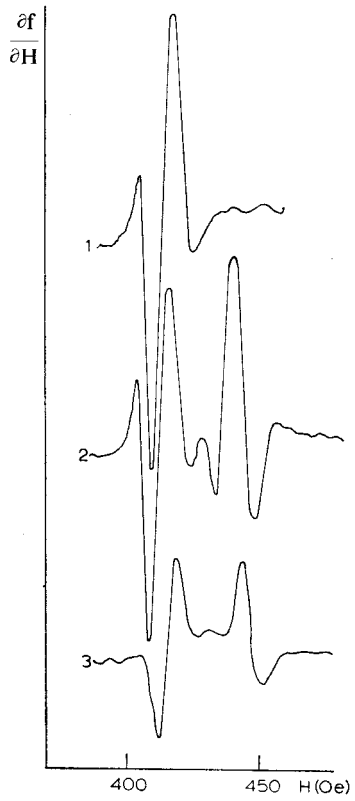

Fig. 19. Splitting of the size effect lines in indium due to a wedge shape of the sample. (1) a size effect line in a plane–parallel shaped sample ($d = 0.4$ mm, $f = 3$ Mc/s, $\boldsymbol{n} \parallel [011]$, $\boldsymbol{H} \parallel [0\bar{1}1]$); (2) the same line in a 5′-wedge shaped sample, ($\Delta d/d = 7\%$); (3) line in the same wedge shaped sample at another direction of the field $\{\sphericalangle(\boldsymbol{H}, [0\bar{1}1]) = 8°\}$. In all three cases, $\boldsymbol{H}$ is parallel to the sample surface.

6) *Smoothness of the surface.* The influence of the surface smoothness upon the size effect lines may be imagined if we assume that the specular scattering of electrons at the surface occurs under some conditions. The specular scattering may be expected, for example, near the left part of the size effect lines in the region $0 \leq (H_0 - H)/H_0 \leq \delta/d$, where effective electrons reach the surface at very small angles. The shape of the lines, however, remains quite

References p. 232

the same when samples with etched surfaces are used instead of samples with cast mirror surfaces. This may be explained either by the complete absence of specular scattering or by the fact that disturbances of the surface smoothness (etch pits) are considerably smaller than the depth of the skin layer. In bismuth the second reason is quite obvious.

7) *Polarization of the electromagnetic field.* Each size effect line in a given sample has its own most advantageous polarization when the electric field is applied along the velocity vector of the electrons at the effective point of the trajectory. Formally the influence of the polarization is related to the fact that the Boltzmann equation (5) as well as eq. (7) contain the electric field in the form of the scalar product $\boldsymbol{E} \cdot \boldsymbol{v}$. For the limiting point size effect, for example, the most advantageous direction of $\boldsymbol{E}$ is along the projection of $\boldsymbol{H}$ on the sample plane (see Fig. 3). As far as the shape of the line is concerned, it remains unchanged as the electric field turns at least within $\pm 60^\circ$ from the most advantageous polarization.

5. Applications of radiofrequency size effects.

One of the possible applications of the size effects actually was already mentioned in the previous section. The size effects presumably may give a valuable information concerning the structure of a high-frequency field in a metal in general, and in the skin layer in particular, in the presence of a constant magnetic field.

In the present section we will expound on the other two applications of the size effects: the study of the shape of the Fermi surfaces and the study of the length of the electron free path.

5.1. Shape of the Fermi surface

The use of size effects makes it possible to obtain various information concerning the Fermi surface. For the sake of convenience we shall divide the following material into several items approximately corresponding to the succession of the discussion of the experimental data.

1) The cutoff effect of the extremal orbit is usually observed when a field is applied parallel to the metal surface. The position of the size effect lines on the scale of the magnetic fields determines, in this case, the calipers of various sections of the Fermi surface. The caliper of the Fermi surface in the $[\boldsymbol{nH}]$ direction, which is of interest to us, is calculated in accordance with eq. (30). The thickness of the sample plate and the intensity of the magnetic field may

be measured with an accuracy up to one per cent. For this reason the determination of the caliper being measured is limited by the arbitrary determination of the H_0 value within the width of the line, i.e. in the final analysis it is limited by insufficient knowledge of the line shape. Formally the H_0 value is known with an accuracy up to the line width Δ_H and, therefore, in such metals as indium and tin the error in measurements of the momentum absolute value does not exceed five per cent. Generally speaking this result is not so bad, if we bear in mind that the absolute measurements are usually not so important as the relative ones (the shift of lines while the field is rotated within the sample plane). In the case of bismuth, however, where just the absolute momentum values are of special interest, Δ_H/H_0 reaches the value 0.25 due to the considerable thickness of the skin layer. Nevertheless, even in this case the measurements are possible if some additional considerations are taken into account during the determination of the H_0 value.

As it was shown in Fig. 18, the line asymmetrically widens as the frequency decreases. Taking into account the mechanism of the line widening discussed in the previous section, we may affirm that the H_0 value to be found is determined by the left edge of the line which does not shift when the frequency changes. The H_0 values determined with the aid of the left minimum of the lines in bismuth samples with thickness 0.97 mm and 1.20 mm gives the magnitude for the momentum along the binary axis $p_1 = 0.54 \times 10^{-22}$ g·cm/sec. This agrees well with the results of measurements carried out with the aid of other methods[41,63]. Using the position of the line central maximum for H_0, we would obtain the value $p_1 = 0.58 \times 10^{-22}$ g·cm/sec, which disagrees with Refs. 41 and 63, and is beyond the possible errors of these works.

Presumably it is thus possible to affirm that for all types of size effects in the H_0 measurements the left (low-field) edge of the size effect line should be used instead of its centre, which has been used in Refs. 49, 52 and 53. It is interesting to note that such a correction removes a three per cent discrepance noted in Ref. 38 between the measurable period ΔH on the plots of the size effect from the open trajectories and the period calculated by the aid of eq. (47) with the reciprocal vector $\boldsymbol{b}$ known from crystallography.

2) Rotating a constant magnetic field within the sample plane, we may obtain the angular dependence of the value H_0 and hence that of the value p with the aid of the relationship (30). This gives us the information on the shape of the corresponding section of the Fermi surface. In some specially symmetrical cases the dependence of p on an angle of turning χ, constructed in

References p. 232

polar coordinates, is the central section of the Fermi surface of a plane normal to $\boldsymbol{n}$. The extremal orbits, however, on which the size effect is observed, may show a variety of shapes and the surfaces themselves may be differently turned relative to $\boldsymbol{n}$. For this reason, in the general case $\boldsymbol{p}$ determines the caliper (in the direction $\chi+\frac{1}{2}\pi$) of the shaded projection of the Fermi surface on the plane perpendicular to $\boldsymbol{n}$ (see Fig. 20). Therefore, strictly speaking the interpretation of the experimental data is usually not unique; some additional considerations such as the nearly-free-electron model would be required for the reconstruction of the Fermi surface.

3) The behaviour of the lines in an inclined magnetic field may give additional information, which is very useful for the interpretation of the experimental data. The linear shift of the line with a tip angle growth shows, for example [according to eq. (31)], that the Fermi surface is inclined relative to the sample surface. This phenomenon was used to study the Fermi surface

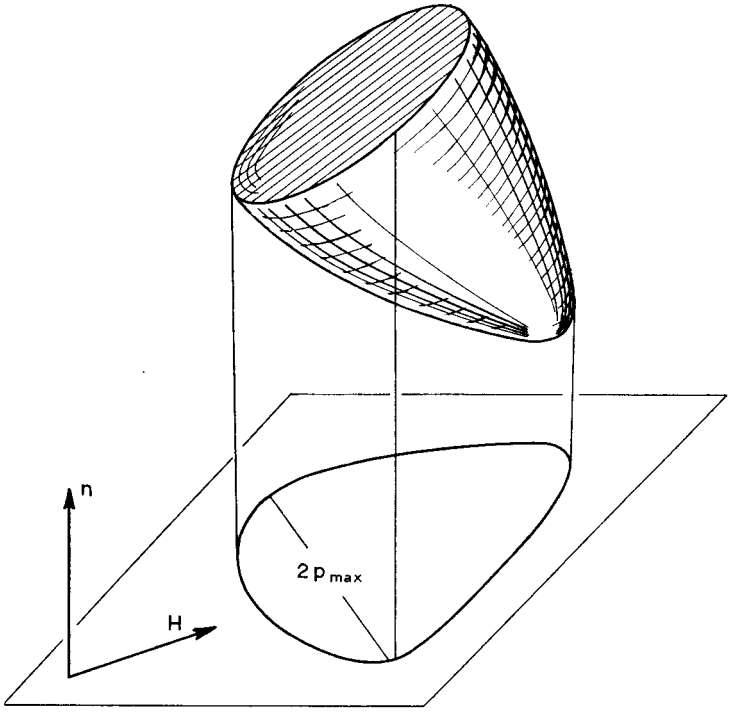

Fig. 20. A measurement of a caliper of a Fermi surface which has a complicated form.

References p. 232

in indium. According to the nearly-free-electron model, the Fermi surface in indium in the third zone should consist of tubes a ong the edges of the Brillouin zone. The study of the behaviour of the lines at the inclinat on made it possible to separate the lines on the tubes from those connected with other sections of the Fermi surface, and to determine in each particular case the position of the tube in the reciprocal lattice.

The split of the size effect lines at the field inclination may be interpreted in two different ways. There may be, for example, two sections of the Fermi surface (e.g., two tubes) which are symmetrically inclined relative to $\boldsymbol{n}$; such a situation was observed in indium (see Ref. 53, line g_2). On the other hand, the split may indicate that the orbit being observed is not the central one [see eqs. (41) and (42)]. In the case of indium such orbits are present in the second zone (see Fig. 15). The behaviour of the appropriate size effect lines was previously illustrated in Fig. 8.

4) The size effect from breaks of the electron trajectories (of course, if it is possible to show that the lines are really connected with the breaks) indicates the presence of sharp edges on the Fermi surface or, to be more precise, the presence of edges with a bend radius $\rho \lesssim (\delta/d)p_0$. In the case of indium this upper limit for $\rho/p_0 \simeq 3\%$. It is interesting how often such sharp edges occur in the Fermi surfaces. It is clear now that the same effect caused by breaks of the electron trajectory had been observed previously in tin also on the square trajectory mentioned above when the diagonal of the square was parallel to the sample surface (Ref. 49, $\boldsymbol{H} \| C_4$, $\boldsymbol{n} \| [110]$, curve 4_2).

5) The presence of the open trajectories may also be shown with the aid of size effects. From the outward appearance of the plots $Z(H)$ some conclusions may be drawn concerning the form of the open trajectories, in particular concerning the existence of the effective points in them.

6) The size effect from the limiting points makes it possible to measure the curvature at certain points of the Fermi surface. In comparison with the measurements of calipers of the extremal orbits, we have here an additional source of errors which is an absolute value of the angle φ of the field inclination contained in (40). Since only the changes of the angle of inclination $\Delta\varphi$ may be measured experimentally, an absolute value of the angle φ should be obtained by linear extrapolation to $\Delta H(\varphi) = 0$. It is assumed that the radius of curvature $K^{-\frac{1}{2}}$ does not depend on φ. If the angular region of the existence of the limiting point is sufficiently large, the curves with opposite

References p. 232

φ signs may be used to increase the accuracy of the determination of the absolute value of the angle φ.

7) The impedance oscillations in the perpendicular magnetic field may be used for detecting helical trajectories with extremal displacement along the field [56].

5.2. Length of the electron free path

From the viewpoint of the possibilities of studying the length of the electron free path in a metal, various types of size effects are probably not of one and the same value. The effect from the extremal orbits in a magnetic field applied parallel to the surface (the cutoff size effect) involves several changes of the number μ of the electron passage piercing the skin layer: to the right of the line at $H > H_0$, $\mu \sim l/\pi d$, to the left of the line $\mu = 1$ and within the width of the line in the case of double-side excitation $\mu \sim 2l/\pi d$. This makes the dependence of the line amplitude on l/d more complicated, especially as the condition $l \gg d$ practically cannot be satisfied in experiments. The size effects related to the drift of a group of electrons from one skin layer to the other, i.e. effects caused by the vicinity of the limiting point, extremal non-central trajectories and open trajectories, are more convenient for the measurements of l. As it was stated above, the line amplitude of these effects contains the factor $e^{-\Lambda/l}$, where Λ is the length of the path from one skin layer to the other. For a limiting point trajectory $\Lambda = d/\sin\varphi$, for an extremal non-central helical trajectory $\Lambda_n \simeq |n - \frac{1}{2}|\pi d$ $(n = 0, 1, 2\ldots)$ [see eq. (41)] and for an open trajectory $\Lambda = kd/\cos\gamma$, where the factor k is used for taking into account the depth of "crimping" of the open trajectory. Such a simple dependence on l is a consequence of the geometry of the experiment: the electron may pass through the second "receiving" skin layer only once even at $l = \infty$. The line amplitude is proportional to the probability that the electron is not scattered in the path Λ. (Strictly speaking the effect caused by breaks of the trajectories also belongs to this group of effects, since in this case the electron may only once pass through the second skin layer.)

The mean free path l may be presented in the form

$$1/l = 1/l_0 + 1/l_{ph}, \tag{49}$$

where l_0 is the free path at $T = 0$ and l_{ph} is the free path connected with the electron–phonon collisions. The most convenient method of measuring the value l_0 gives us the limiting point size effect: by changing the tip angle φ we change Λ. A simple mathematical treatment of the dependence of the amplitude $A(\varphi)$ measured at approximately the same values of H makes it

possible to obtain at once l_0. Such measurements were carried out in tin for two different limiting points with the use of the same sample and in the same region of directions of the magnetic field H (Ref. 38). The ratio of the l_0 values was approximately four and the obtained values of l_0 were compared with effective masses and Fermi velocities of electrons at the limiting points.

The measurements of the average value of l_0 along the extremal non-central orbits require the comparison of line amplitudes corresponding to different Λ_n at a certain direction of the magnetic field. Such measurements were performed in Ref. 51. Measurements of l_0 on open trajectories require changes of samples, which is less convenient and gives lower accuracy.

Turning to the problem of the temperature dependence of the free path, it is necessary to emphasize first the principal difference between collisions of electrons with static defects and electron–phonon collisions at low temperatures. This difference becomes important under anomalous skin effect conditions[27]. Electron scattering on static imperfections of the lattice causes deflections through large angles as often as deflections through small angles[8] – the scattering is an isotropic one. For this reason a single act of scattering exerts the same influence upon both the static conductivity and the size effect. On the other hand the interaction of an electron with vibrations of the lattice is influenced by the fact that the electron may emit or absorb a phonon. When the temperature $T<\theta_D$ (θ_D is the Debye temperature) the electron will scatter only through the small angle

$$\beta \simeq p_{ph}/p_0 \simeq T/\theta_D,$$

where p_{ph} is the average absolute value of the phonon momentum at the temperature T and p_0 is the curvature radius of the Fermi surface. The effectiveness of such a scattering varies from case to case. In the static conductivity, $(T/\theta_D)^2$ collisions are required for an essential scattering of the electron by the phonons, since only after such a number of collisions the electron scatters through the angle of unit order. As a result the supplementary factor of T^2 is introduced into the temperature dependence of the static resistance ρ (as it is known, $\rho \sim T^5$ and the factor of T^3 is determined, roughly speaking, by the dependence of the number of phonons on T). In the case of size effects, the scattering through a small angle may be sufficient for the conversion of the electron into an ineffective one due to the small skin layer thickness δ. The value of this angle η and hence the value l_{ph} depend on the type of effect, the relation δ/d, and even on the value of the magnetic field. Let us estimate, for example, η for the case of the limiting point[64]. The path L which an effective electron may travel in the skin layer amounts

approximately to $L \simeq \delta^{\frac{1}{3}} d^{\frac{2}{3}} \varphi^{-1} n^{-\frac{2}{3}}$ [see Fig. 3 and p. 91]; $n(H)$ is the number of the line showing the number of revolutions made by the electrons. A considerable reduction in this path occurs in the case of scattering through the angle δ/L. Thus,

$$\eta = \delta/L = (n\delta/d)^{\frac{2}{3}}. \tag{50}$$

In actual experiments carried out int in with $\delta_{\text{eff}} \sim 10^{-4}$ cm (and $\delta \sim 10^{-3}$ cm evaluated from the line width), $d = 4 \times 10^{-2}$ cm, $\varphi \sim 10^{-1}$ and $n = 2$, $\eta \sim 10^{-3}$ was obtained. At the same time, at helium temperatures the interaction of an electron with a phonon in tin deflects the electron through an angle of the order of 10^{-2}. The difference between η and this angle of deflection amounting to one order of magnitude is certainly small, but, as it may be considered from these estimates, even a single collision is sufficient for making an electron ineffective. For this reason the dependence of l_{ph} on the temperature should be proportional in this case to T^3, but not to T^5, and this phenomenon was observed experimentally[64].

As it is shown in (50), a dependence $l_{\text{ph}}(H)$ is also possible. Since at large values of n (i.e. in large fields) η increases, then at $n \gg 1$ several collisions may be required to make an electron ineffective. This problem, however, is not yet studied sufficiently. Some attempts were made also to apply the effect of the cutoff type to the study of the temperature dependence $l(t)$ (see Refs. 32 and 64). These attempts proved not to be very successful, probably due to the difficulties mentioned above in the interpretation of the results.

In both experiments, however, in tin and gallium, various temperature dependences of the amplitude were observed for various lines and this indicates the dependence of l_{ph} on the position of the extremal orbit on the Fermi surface.

Acknowledgements

The author is very much indebted to Prof. Yu. V. Sharvin, Dr. É. A. Kaner and Mr. I. P. Krylov for valuable discussions while writing this article.

Note added in proof. Since the article was written a number of new works[65–69] have been done in the field of radiofrequency size effects. We shall restrict ourselves here to enumeration of new results:

Ref. 65–a RF size effect from a chain of trajectories was observed in rubidium. Inclination of the magnetic field amplified the lines for which the conditions (33)–(35) were satisfied. So the mechanism of a weak damping chain predicted by Kaner[37] was detected experimentally.

References p. 232

Ref. 66–a RF size effect was observed in potassium. Inclination of the magnetic field led to a line shift toward higher fields just in accordance with eqs. (43)–(45) and Fig. 14. At tip angles $\varphi \gtrsim 25°$ the size effect lines disappeared.

Ref. 67 – the shape of the limiting point size effect line was computed. The results are in good agreement with experimental curves[62].

Ref. 68 – a RF size effect was observed in cadmium. It was used for an investigation of the Fermi surface.

Ref. 69 – a RF size effect was observed in aluminium.

Thus RF size effects of different types have been observed so far in Al[69], Bi[50], Cd[59,68], Ga[32], In[53,62], K[66], Rb[65], Sn[38,49] and W[44].

REFERENCES

Reports and monographs

[1] I. M. Lifshitz and M. I. Kaganov, Usp. Fiz. Nauk **69,** 419 (1959) [English transl.: Soviet Phys.-Usp. **2,** 831 (1960)].

[2] I. M. Lifshitz and M. I. Kaganov, Usp. Fiz. Nauk **78,** 411 (1962) [English transl.: Soviet Phys.-Usp. **5,** 878 (1963)].

[3] I. M. Lifshitz and M. I. Kaganov, Usp. Fiz. Nauk **87,** 389 (1965) [English transl.: Soviet Phys.-Usp. **8,** 805 (1966)].

[4] E. H. Sondheimer, Advan. Phys. **1,** 1 (1952).

[5] A. B. Pippard, Advan. Electron. Electron Phys. **6,** 1 (1954).

[6] A. B. Pippard, Rept. Progr. Phys. **23,** 176 (1960).

[7] M. Ya. Azbel' and I. M. Lifshitz, Progress in Low Temperature Physics, Vol. 3, Ed. C. J. Gorter (North-Holland Publishing Co., Amsterdam, 1961) p. 288.

[8] R. E. Peierls, Quantum Theory of Solids (Oxford at the Clarendon Press, 1955).

Original papers

[9] K. Fuchs, Proc. Cambridge Phil. Soc. **34,** 100 (1938).

[10] E. R. Andrew, Proc. Phys. Soc. (London) A **62,** 77 (1949).

[11] D. K. C. MacDonald, Proc. Phys. Soc. (London) A **63,** 290 (1950).

[12] E. H. Sondheimer, Phys. Rev. **80,** 401 (1950).

[13] J. Babiskin and P. G. Siebenmann, Phys. Rev. 107, 1249 (1957).

[14] N. H. Zebouni, R. E. Hamburg and H. J. Mackey, Phys. Rev. Letters **11,** 260 (1963).

[15] Yu. V. Sharvin and L. M. Fisher, Zh. Eksperim. i Teor. Fiz. Pis'ma **1** (5), 54 (1965) [English transl.: JETP Letters **1,** 152 (1965)].

[16] A. B. Pippard, Proc. Roy. Soc. (London) A **191,** 385 (1947).

[17] A. B. Pippard, Proc. Roy. Soc. (London) A **224,** 273 (1954).

[18] G. E. H. Reuter and E. H. Sondheimer, Proc. Roy. Soc. (London) A **195,** 336 (1948).

[19] R. G. Chambers, Proc. Phys. Soc. (London) A **65,** 458 (1952).

[20] A. B. Pippard, G. E. H. Reuter and E. H. Sondheimer, Phys. Rev. **73,** 920 (1948).

[21] A. B. Pippard, Proc. Roy. Soc. (London) A **203,** 98 (1950).
[22] R. G. Chambers, Proc. Roy. Soc. (London) A **215,** 481 (1952).
[23] G. E. Smith, Phys. Rev. **115,** 1561 (1959).
[24] P. N. Dheer, Proc. Roy. Soc. (London) A **260,** 333 (1961).
[25] E. W. Johnson and H. H. Johnson, J. Appl. Phys. **36,** 1286 (1965).
[26] M. Ya. Azbel' and É. A. Kaner, Zh. Eksperim. i Teor. Fiz. **32,** 896 (1957) [English transl.: Soviet Phys.-JETP **5,** 730 (1957)].
[27] M. Ya. Azbel' and É. A. Kaner, Phys. Chem. Solids **6,** 113 (1957).
[28] M. Ya. Azbel', Zh. Eksperim. i Teor. Fiz. **39,** 400 (1960) [English transl.: Soviet Phys.-JETP **12,** 283 (1961)].
[29] I. M. Lifshitz, M. Ya. Azbel' and M. I. Kaganov, Zh. Eksperim. i Teor. Fiz. **31,** 63 (1956) [English transl.: Soviet Phys.-JETP **4,** 41 (1957)].
[30] M. S. Khaikin, Zh. Eksperim. i Teor. Fiz. **39,** 212 (1960) [English transl.: Soviet Phys.-JETP **12,** 152 (1961)].
[31] V. F. Gantmakher and Yu. V. Sharvin, Zh. Eksperim. i Teor. Fiz. **39,** 512 (1960) [English transl.: Soviet Phys.-JETP **12,** 358 (1961)].
[32] J. F. Cochran and C. A. Shiffman, Phys. Rev. **140,** A 1678 (1965).
[33] V. Heine, Phys. Rev. **107,** 431 (1957).
[34] É. A. Kaner, Dokl. Akad. Nauk SSSR **119,** 471 (1958) [English transl.: Soviet Phys.-Doklady **3,** 314 (1958)].
[35] M. S. Khaĭkin, Zh. Eksperim. i Teor. Fiz. **41,** 1773 (1961) [English transl.: Soviet Phys.-JETP **14,** 1260 (1962)].
[36] V. F. Gantmakher, Zh. Eksperim. i Teor. Fiz. **43,** 345 (1962) [English transl.: Soviet Phys.-JETP **16,** 247 (1963)].
[37] É. A. Kaner, Zh. Eksperim. i Teor. Fiz. **44,** 1036 (1963) [English transl.: Soviet Phys.-JETP **17,** 700 (1963)].
[38] V. F. Gantmakher and É. A. Kaner, Zh. Eksperim. i Teor. Fiz. **45,** 1430 (1963) [English transl.: Soviet Phys.-JETP **18,** 988 (1964)].
[39] C. C. Grimes, A. F. Kip, F. Spong, R. A. Stradling and P. Pincus, Phys. Rev. Letters **11,** 455 (1963).
[40] M. S. Khaĭkin, Pribory i Tekhn. Eksperim. **3,** 95 (1961) [English transl.: Instr. Exptl. Tech. (USSR) (1962)].
[41] M. S. Khaĭkin and V. S. Edel'man, Zh. Eksperim. i Teor. Fiz. **47,** 878 (1964) [English transl.: Soviet Phys.-JETP **20,** 587 (1965)].
[42] R. T. Mina and M. S. Khaĭkin, Zh. Eksperim. i Teor. Fiz. **48,** 111 (1965) [English transl.: Soviet Phys.-JETP **21,** 72 (1965)].
[43] W. M. Walsh, Jr. and C. C. Grimes, Phys. Rev. Letters **13,** 523 (1964).
[44] W. M. Walsh, Jr., C. C. Grimes, G. Adams and L. W. Rupp, Jr., Proc. IXth Intern Conf. Low Temp. Phys., Columbus, Ohio, 1964 (Plenum Press, New York, 1965) part B, p. 765.
[45] R. B. Lewis and T. R. Garver, Phys. Rev. Letters **12,** 693 (1964).
[46] S. Schultz and C. Latham, Phys. Rev. Letters **15,** 148 (1965).
[47] M. S. Khaĭkin, Zh. Eksperim. i Teor. Fiz. **43,** 59 (1962) [English transl.: Soviet Phys.-JETP **16,** 42 (1963)].
[48] V. F. Gantmakher, Zh. Eksperim. i Teor. Fiz. **42,** 1416 (1962) [English transl.: Soviet Phys.-JETP **15,** 982 (1962)].
[49] V. F. Gantmakher, Zh. Eksperim. i Teor. Fiz. **44,** 811 (1963) English transl.: Soviet Phys.-JETP **17,** 549 (1963).

[50] V. F. Gantmakher, Zh. Eksperim. i Teor. Fiz. Pis'ma **2,** 557 (1965) [English transl.: JETP Letters **2,** 346 (1965)].
[51] V. F. Gantmakher and I. P. Krylov, Zh. Eksperim. i Teor. Fiz. **47,** 2111 (1964) [English transl.: Soviet Phys.-JETP **20,** 1418 (1965)].
[52] V. F. Gantmakher, Zh. Eksperim. i Teor. Fiz. **46,** 2028 (1964) [English transl.: Soviet Phys.-JETP **19,** 1366 (1964)].
[53] V. F. Gantmakher and I. P. Krylov, Zh. Eksperim. i Teor. Fiz. **49,** 1054 (1965) [English transl.: Soviet Phys.-JETP **22,** 734 (1966)].
[54] É. A. Kaner and V. L. Fal'ko, Zh. Eksperim. i Teor. Fiz. **49,** 1895 (1965) [English transl.: Soviet Phys.-JETP **22,** 1294 (1966).]
[55] C. C. Grimes and A. F. Kip, Phys. Rev. **132,** 1991 (1963).
[56] V. F. Gantmakher and É. A. Kaner, Zh. Eksperim. i Teor. Fiz. **48,** 1572 (1965) [English transl.: Soviet Phys.-JETP **21,** 1053 (1965)].
[57] J. F. Koch and A. F. Kip, Phys. Rev. Letters **8,** 473 (1962).
[58] W. M. Walsh, Jr., Phys. Rev. Letters **12,** 161 (1964).
[59] A. A. Maryakhin and V. P. Nabereshnykh, Zh. Eksperim. i Teor. Fiz. Pis'ma **3,** 205 (1966) [English transl.: JETP Letters **3,** 130 (1966)].
[60] M. Ya. Azbel', Phys. Chem. Solids **7,** 105 (1958).
[61] I. P. Krylov, Zh. Eksperim. i Teor. Fiz. Pis'ma **1,** 4, 24 (1965) [English transl.: JETP Letters **1,** 116 (1965)].
[62] I. P. Krylov and V. F. Gantmakher, Zh. Eksperim. i Teor. Fiz. **51,** 740 (1966) [English transl.: Soviet Phys.-JETP **24** (1967)].
[63] A. P. Korolyuk, Zh. Eksperim. i Teor. Fiz. **49,** 1009 (1965) [English transl.: Soviet Phys.-JETP **22,** 701 (1966)].
[64] V. F. Gantmakher and Yu. V. Sharvin, Zh. Eksperim. i Teor. Fiz. **48,** 1077 (1965) [English transl.: Soviet Phys.-JETP **21,** 720 (1965)].
[65] P. S. Peercy and W. M. Walsh, Jr., Phys. Rev. Letters **17,** 741 (1966).
[66] J. F. Koch and T. K. Wagner, Report at the Xth Intern. Conf. Low Temp. Phys., Moscow, 1966.
[67] E. A. Kaner and V. L. Fal'ko, Report at the Xth Intern. Conf. Low Temp. Phys., Moscow, 1966.
[68] V. P. Nabereshnykh and A. A. Maryakhin, Report at the Xth Intern. Conf. Low Temp. Phys., Moscow, 1966.
[69] J. F. Koch and T. K. Wagner, Bull. Am. Phys. Soc. **11,** 170 (1966).